

UCSF

UC San Francisco Electronic Theses and Dissertations

Title

Evaluation of Enamel Demineralization and Remineralization Using Near Infrared Imaging

Permalink

<https://escholarship.org/uc/item/0c57x29h>

Author

Trinh, Peter Quoc

Publication Date

2010

Peer reviewed|Thesis/dissertation

Evaluation of Enamel Demineralization and Remineralization Using Near Infrared Imaging

by

Peter Quoc Trinh

THESIS

Submitted in partial satisfaction of the requirements for the degree of

MASTER OF SCIENCE

in

Oral and Craniofacial Sciences

in the

GRADUATE DIVISION

of the

UNIVERSITY OF CALIFORNIA, SAN FRANCISCO

Acknowledgements

I would like to thank my committee members, Dr. Daniel Fried, Dr. Arthur Miller and Dr. Michal Staninec for their support and guidance. I want to thank Dr. Fried for being a great mentor and for giving me the opportunity to work in his lab. I would like to thank Dr. Miller for the hours of critique and the constant guidance and interest in my project. I would have not been able to stay on top of the work without his support. Dr. Staninec, many thanks for the guidance and feedback. My last thank goes to Dr. Jennifer Wu for paving the way and for giving me support and making me laugh over the years. I would not have been able to complete my project without her constant help.

Abstract

PURPOSE: The study uses near-infrared imaging at 1310 nm to acquire high contrast images of early enamel demineralization and subsequent remineralization (i.e. “white spot lesions” and “remineralized lesions”). The specific aims are: 1) to test the hypothesis that we can measure differences in optical contrast at 1310 nm between sound and artificially demineralized/remineralized enamel on the buccal and occlusal surfaces of teeth; and 2) to test the hypothesis that NIR imaging manifests greater contrast than other methods, such as qualitative light fluorescence and cross-polarization visible reflectance.

METHODS: 16 human tooth samples were used in this study. Teeth were painted with a clear varnish, leaving a 2x2 window on the buccal and occlusal surfaces for demineralization. Teeth were imaged with the following methods: Transillumination - NIR with polarization; reflected light - NIR with cross polarization; Quantitative Light Fluorescence; and reflected light after periods of demineralization and remineralization.

RESULTS: All of the imaging techniques showed an increase in contrast during the demineralization periods and the remineralization periods. NIR imaging with cross polarization offered the highest contrast during the periods of demineralization and a decrease during the remineralization but did not statistically differ from the other methods.

CONCLUSIONS: NIR imaging can detect demineralization and remineralization in enamel. It can become a useful tool in for non destructive monitoring of white spot lesions during orthodontic treatment.

TABLE OF CONTENTS

Abstract Pages.....	iv
Introduction.....	1
Demineralization.....	1
Visible Light.....	7
Quantitative Light Fluorescence (QLF).....	9
Near Infrared Imaging.....	10
Polarized Sensitive Optical Coherence Tomography.....	11
Purpose.....	12
Specific Aims.....	12
Materials and Methods.....	13
A. Sample Preparation.....	13
1. Sample Acquisition and Mounting.....	13
2. Fiducial Marking.....	13
3. Enamel Varnish Application.....	14
B. Demineralization/Remineralization Challenge.....	14
1. Demineralization.....	14
2. Remineralization.....	15
C. Methods of Imaging.....	15
1. Transillumination.....	15-16
2. Reflected Light NIR with Polarization.....	17
3. QLF.....	17-18
4. Reflected Light Visible with Polarization.....	18-19
D. Method of Imaging Analysis.....	19
1. PS-OCT.....	20
2. PS-OCT Line Profile.....	21
Results.....	22
A. Buccal Images.....	22-31
B. Occlusal Images.....	32-38
Discussion.....	39-42
Conclusion.....	42-43

TABLE OF CONTENTS

Appendices.....	44
A. Appendix A: Buccal Images	46
Sample 1.....	47
Sample 2.....	48
Sample 3.....	49
Sample 4.....	50
Sample 5.....	51
Sample 6.....	52
Sample 7.....	53
Sample 8.....	54
Sample 9.....	55
Sample 10.....	56
Sample 11.....	57
Sample 12.....	58
Sample 13.....	59
Sample 14.....	60
Sample 15.....	61
Sample 16.....	62
B. Appendix B: Occlusal Images	63
Sample 1.....	64
Sample 2.....	65
Sample 3.....	66
Sample 4.....	67
Sample 5.....	68
Sample 6.....	69
Sample 7.....	70
Sample 8.....	71
Sample 9.....	72
Sample 10.....	73
Sample 11.....	74
Sample 12.....	75
Sample 13.....	76
Sample 14.....	77

TABLE OF CONTENTS

Sample 15.....	78
Sample 16.....	79

List of Tables

Courtesy of Fried Laboratories

Table 1 Comparison T0 Buccal	27
Table 2 Comparison D4 Buccal	28
Table 3 Comparison R2 Buccal	30
Table 4 OCT Values Buccal	31
Table 5 Comparison T0 Occlusal	35
Table 6 Comparison D4 Occlusal	36
Table 7 Comparison R2 Occlusal	37
Table 8 OCT Values Occlusal	38

List of Figures

Courtesy of Fried Laboratories

Figure 1. Visible Light A) Buccal Setup B) Occlusal Setup	9
Figure 2. QLF A) Buccal Setup B) Occlusal Setup	10
Figure 3 NIR Reflectance A) Buccal Setup B) Occlusal Setup	10
Figure 4 NIR Transillumination Occlusal Setup	11
Figure 5 Fiducial markings on A) Buccal and B) Occlusal Surfaces	14
Figure 6. Demineralization A) Buccal and B) Occlusal	15
Figure 7 NIR Transillumination Occlusal Surface	16
Figure 8 NIR Reflectance A) Buccal B) Occlusal Surfaces	17
Figure 9 QLF A) Buccal and B) Occlusal Surface	18
Figure 10 Visible A) Buccal and B) Occlusal Surface	19
Figure 11 Line Profile	20
Figure 12 PS-OCT Line Profile taken through demineralized region	21
Figure 13 Comparison of NIR Reflectance Time Points Buccal	23
Figure 14 Comparison of NIR Transillumination Time Points Buccal	24
Figure 15 Comparison of QLF Time Points Buccal	25
Figure 16 Comparison of Visible Light Time Points Buccal	26
Figure 17 Comparison of T0 Buccal Surface	27
Figure 18 Comparison of D4 Buccal Surface	29
Figure 19 Comparison of R2 Buccal Surface	30
Figure 20 Comparison of NIR Reflectance Time Points Occlusal	32
Figure 21 Comparison of QLF Time Points Occlusal	33
Figure 22 Comparison of Visible Light Time Points Occlusal	34
Figure 23 Comparison of T0 Occlusal Surface	35
Figure 24 Comparison of D4 Occlusal Surface	36
Figure 25 Comparison of R2 Occlusal Surface	37

Introduction

Demineralization

The etiology of demineralization and caries is complex and involves the tooth structure, dental biofilm, dietary factors, genetic factors and a multitude of environmental factors. The disease is communicable with parents and caregivers often infecting the infants that they care for[1]. Oral bacteria combined with fermentable carbohydrates produce acids that demineralize tooth structure. The dissolved mineral content of the tooth is then carried away from the tooth surface by the saliva in the oral cavity. The bacteria and acids travel down the weakened tooth surface and once the dento-enamel junction is reached the lesion spreads rapidly due to the solubility and high permeability of dentin. If this process is continued uncontrolled then the tooth structure weakens and becomes cavitated [2].

Demineralization of tooth structure is a result from an imbalance between mineral content of the tooth surface and saliva contained in the oral cavity. Minerals are constantly exchanged between the tooth surface and the saliva. This process is controlled by bacterial challenge that favors demineralization, and resistance factors that favors remineralization, of the tooth[3]. If demineralization progresses significantly then the tooth becomes cavitated. There has been significant work that has contributed to our understanding of the caries process. Mainly that it is a chronic, dietomicrobial disease caused from a shift in the remineralization and demineralization of tooth surface [2].

The crowns of teeth are covered with enamel, which is the hardest tissue in the human body. It is composed of 92-96% inorganic mineral and 4% organic material. The

mineral is composed of mainly calcium phosphate in the form of hydroxyapatite crystals which can be carbonated or fluoridated. The enamel crystals are organized into rods which are arranged perpendicular to the tooth surface. The crystals are 30-40 nm in diameter and can be up to 10nm in length [15]. As a result of the orientation and composition of the dental rods the scattering of light is dependent on the source of light in relationship to the orientation of the enamel rods. During enamel demineralization the dissolution of the mineral content creates pores that highly scatter light[4]. This phenomenon is responsible for the appearance of white spot lesions.

Early carious lesions in the enamel present as white spot lesions. The area is slightly softer than sound enamel. The phenomenon is caused by a change in the optical properties of the demineralized enamel. There is an increase in light scattering which causes the demineralized area to appear white. There is an increase in whiteness when the area is dried[5]. The surface softening is caused mainly by mineral loss in the interprismatic substance that forms the enamel rods. If mineral loss continues then a subsurface lesion forms. This lesion is characterized by dissolution of mineral content in the deeper part of the enamel while maintaining an intact surface layer. A porous but mineral rich layer covers the hypomineralized body of the lesion[5].

The role of bacteria and the formation of dental caries is traced back to the studies done by Clarke and his discovery of *S. mutans* in the oral cavity. It has since been determined that the human mouth harbors a complex ecosystem of bacteria. Many of these bacteria are acid-producing. They receive their nourishment from fermenting

carbohydrates ingested from the host. Some of these bacteria include: *S. mutans*, *S. anginosus*, *S. constellatus*, *S. gordonii*, *S. intermedius*, *S. mitis*, *S. oralis*, *S. salivarius*, and *S. sanguis* [6]. These bacteria produce acids that dissolve soft tissue along with extracellular polysaccharides that help them adhere to tooth structure. [7].

The virulence of *S. mutans* is due to many factors. It is a facultative anaerobe which allows it to live anywhere in the oral cavity under both oxygen rich and deficient environments. It can ferment a multitude of sugars and sugar alcohols present in food such as: glucose, sucrose, lactose, trehalose, mannitol, sorbitol, raffinose, and melibiose[8].

Biofilm formation occurs in stages. The first stage involves formation of an acquired enamel pellicle (AEP) on the surface of the tooth structure. This coating is created from bacteria that include synthesized polysaccharides such as glucans and fructans. The second stage involves adherence of bacteria to the AEP. The final stage involves proliferation of the bacteria and where the bacterial community in the biofilm has reached a steady state[9].

Biofilm is the layer of organisms, their by-products and food debris that coats the tooth surface. It is home to hundreds of types of bacteria. The main bacteria of concern that cause demineralization are the acid tolerant and acid producing bacteria. *S. mutans* has been shown to be the main culprit in demineralization. Other bacteria implicated in

the demineralization process belong to the *streptococcus* and *lactobacilli* families. These bacteria can ferment most sugars found in the oral cavity such as sucrose, fructose, lactose et [7].

White spot lesions are due to demineralization of the enamel surface: and is the first detectable stage of dental caries. If allowed to progress the tooth will undergo subsequent stages to lesion, cavitation and eventually tooth loss if surgical intervention is not performed[7]. Demineralization of hard tissue in the oral cavity is a dynamic process. Hard tissue undergoes cycles of demineralization and remineralization where the tooth loses and gains mineral content. When the pH drops below a threshold level the mineral content will demineralize from the surface of the tooth. This causes a change in the mineral content of the tooth structure and a change in the optical properties of the tooth.

As the demineralization progresses into dentin the surface layer cavitates which usually warrants surgical intervention [1]. Before the lesion becomes cavitated, the demineralization can be arrested and remineralized. Demineralization and remineralization of tooth structure is a cyclical process dependent on the buffering capabilities of saliva and the demineralization cycles [1]. If the lesions are detected early they can be arrested and reversed by many non surgical, non invasive techniques.

The treatment techniques used to control demineralization include: antibacterial rinses, fluoride treatments, dietary changes/modification, oral hygiene instruction all in

attempt to remineralize the decay before cavitation occurs[10]. The oral environment must be shifted to an environment that favors remineralization. The most efficacious techniques used involve patient education. Decreasing the frequency of carbohydrate consumption, controlling plaque accumulation, increasing salivary flow, altering the oral flora and patient education all help prevent and control demineralization. Therapy includes agents that control bacteria such as chlorhexadine and fluoride to aid in remineralization of tooth structure[1].

Hygiene and diet are key factors in demineralization and formation of caries. Consumption of fermentable carbohydrates has been linked to an increase caries incidence in urbanized societies. This is due to the replacement of crude sugars with refined sugars[11]. Decreasing the frequency of consumption of refined sugars can decrease the amount of demineralization episodes and favor remineralization of hard tissue. Frequent brushing and flossing help remove plaque and bacteria that have accumulated on tooth structure. Fluoride is a mineral that aids in remineralization of tooth structure. Fluoroapatite is the mineral that forms when fluoride is incorporated into the tooth surface. It is also less soluble and more resistant to demineralization. Fluoride also has the additional benefit of inhibiting bacterial metabolism. Chlorhexadine rinses along with antibiotic therapy can also help eliminate the bacteria that cause demineralization in the oral cavity.

The risks and benefits of orthodontic treatment should be carefully measure and weighed. Some of the complications associated with orthodontic treatment are white spot lesions. Critical before orthodontic treatment is patient selection. It is imperative that the patients beginning orthodontic treatment are caries free and present with good oral hygiene. Enamel demineralization on the smooth surfaces of teeth is a common orthodontic complication. Orthodontic appliances provide retention areas for plaque and bacteria leading to potential white spot lesions. In severe cases frank cavitation occurs which requires surgical intervention[12].

O'Reilly and Featherstone have shown that demineralization can appear within one month adjacent to orthodontic brackets in patients who use fluoride containing toothpaste twice daily. Teenagers were at a higher risk of demineralization than adults [13]. Studies have reported an prevalence of 2-96%[14]. These white spot lesions are irreversible and unaesthetic. If the white spot lesions become serious enough they can lead to discontinuation of orthodontic treatment and non-ideal occlusion and aesthetic result.

Caries activity cannot be determined by one single time point. It must be monitored over time to evaluate if the lesion is progressing or arrested and remineralized. Mineral loss associated with caries can be arrested and reversed but only before cavitation takes place. Radiographic evaluation along with clinical evaluation is used to determine the extent of the lesion and subsequent treatment modalities.

Longitudinal assessment of the decalcification is necessary to determine if the lesion is progressing or arrested. It is also necessary to determine if prescribed non invasive therapy has been effective in arresting and remineralizing the decalcification.

Traditional methods used to assess decalcification employ dental probes and radiographs[1]. These traditional techniques however are not sensitive in measuring the depth of the early decalcification. Due to the radiation exposure needed to produce radiographs, this technique is not recommended in monitoring the progression of decalcification. They also lack the sensitivity in detecting early decalcification and are more efficacious in detecting cavitated lesions[15]. Therefore, more sensitive, non-harmful techniques at detecting decalcification are needed. Other diagnostic tools are emerging with better sensitivity to imaging demineralization.

The optical properties of tooth enamel change as a result of demineralization. Imaging techniques that exploit these properties have considerable promise for detection and monitoring of decalcification[4]. Some of these emerging technologies include: Quantitative Light Fluorescence, Near Infra-Red Imaging, Polarized Sensitive Optical Coherence Tomography and Visible Imaging [1].

Visible Light

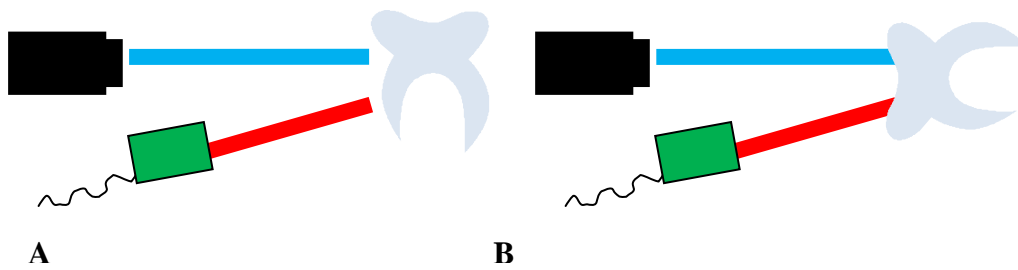
Clinical photographs are a reliable way of recording the appearance of enamel before and after orthodontic treatment. The photographs can be used as a record for the

progression of white spot lesions and to measure any iatrogenic damage done to the tooth during orthodontic treatment. Benson et al found that measurements of enamel demineralization using images from a digital camera are accurate and reproducible[15]. The white spot lesions can also be differentiated from developmental defects of the enamel using photographs. Developmental lesions were found to appear whiter, have a higher luminescence, and were more round in shape than white spot lesions. White spot lesions tend to follow the shape and boundaries of orthodontic brackets[16]. This approach is highly dependent on clinical experience and is subjective assessment.

Photographs are routinely used in clinic to capture pre and post orthodontic treatment. They are cheap and easy to produce. Photographs however introduce systematic error due to the light scatter from the camera flash[17]. Scattered light from the camera flash can be reduced using cross polarization filters. Cross polarization filters placed over the camera lens prevents scattered light from obscuring the image of the white spot lesion. They reduce the amount of reflected light and they improve the quality of the photographs. Filters aid in the clinical assessment of white spot lesions from photographic images[15].

The visible spectrum is between 400-700nm and is used to image teeth in photographs. The main problem using visible light to image caries is the amount of light scattering off the surface of the enamel. Sound enamel obscures light transmission through the teeth and limits the quality of images obtained by using visible light[18].

Figure 1. Visible Light A) Buccal Setup B) Occlusal Setup



Quantitative Light Fluorescence

Quantitative Light fluorescence is a reliable way to image smooth surface demineralization due to the image contrast between sound and demineralized enamel. The fluorescence radiance of demineralized enamel is reduced in comparison to sound enamel. When the image is digitized the fluorescence of the lesion can be quantified in comparison to the sound enamel. The demineralized lesion attenuates the fluorescent signal thus causing the lesion to appear dark[19]. Halfstrom-Bjorkman et al. established a relationship between the mineral loss of a lesion and the amount of fluorescence. Thus QLF can be used to monitor lesion progression of smooth surfaces[20].

The differences in fluorescence intensities of demineralized enamel can be measured over time to longitudinally monitor the progression of a lesion. It can also be used to monitor if a lesion has been arrested in remineralized.

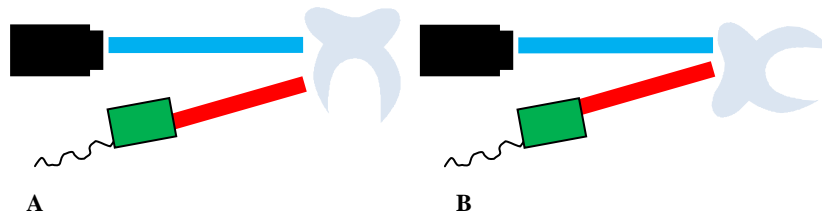


Figure 2. QLF A) Buccal Setup B) Occlusal Setup

NIR

Previous studies have shown that there is an increase in light scattering correlated to mineral loss in enamel caries. The scattering increases in two orders of magnitude at 1310nm[21]. Sound enamel is the most transparent at 1310nm. This allows NIR to be ideally suited to image demineralization of tooth structure.

NIR Reflectance Setup

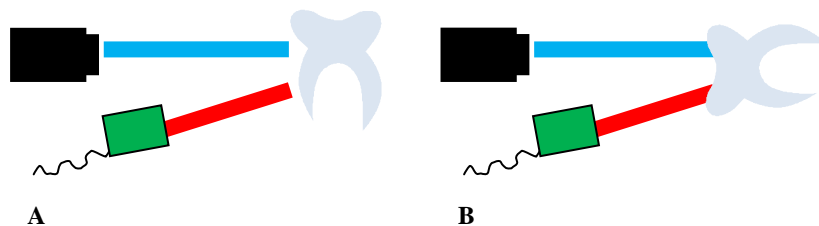


Figure 3. NIR Reflectance A) Buccal Setup B) Occlusal Setup

NIR Occlusal Setup

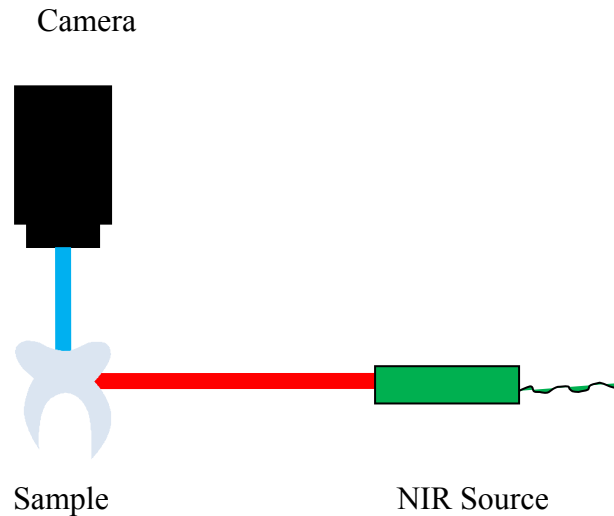


Figure 4. NIR Transillumination, Occlusal Setup

PS-OCT

Optical coherence tomography (OCT) is both nondestructive and noninvasive technique for creating images of internal biological structure of teeth. The imaging technique creates cross-sectional images of the tooth. Polarization-sensitive OCT (PS-OCT) at 1310 nm has been shown to be effective in imaging dental caries and early lesions[21]. It is useful to have imaging tools that can assess the severity of demineralization and remineralization of tooth surfaces. The clinician can use these tools to determine if the lesion is active and progressing or if it is arrested and has undergone remineralization. Recent studies have shown that PS-OCT can be used to measure the depth of lesions and to determine if they have been arrested by the application of topical fluoride[22].

PS-OCT scans were used to acquire tomographic images of the lesions produced in each window. PS-OCT was used in place of microradiography or polarized light microscopy to provide an indication of the lesion depth and severity and verify the lesion is intact. Although it is also a nondestructive imaging technique, it was not one of the four imaging methods compared in this study. PS-OCT is capable of determining the lesion depth and severity nondestructively without thin sectioning and destruction of the tooth.

Purpose

The purpose of this study is to use near infrared imaging at 1310 nm to acquire contrast images of demineralization and remineralization of enamel tissue.

Specific Aims

The specific aims are to:

- 1) to test the hypothesis that we can measure differences in optical contrast at 1310 nm between sound and artificially demineralized/remineralized enamel on the buccal and occlusal surfaces of teeth
- 2) To test the hypothesis that NIR imaging manifests greater contrast than other methods, such as qualitative light fluorescence and visible reflectance with cross-polarization.

Materials and Methods

A. Sample Preparation

1. Sample Acquisition and Mounting

Human teeth (n=18) were collected from UCSF oral surgery department and stored in 1% Thymol solution. Posterior human teeth including premolars and molars were collected and used for the study. The teeth were then sterilized using gamma radiation. Previous studies have shown that sample sizes between 10 and 20 are sufficient to detect significant differences between groups[19]. Buccal and Occlusal surfaces would be experimented on in this study. The surfaces were polished with five micron aluminum oxide slurry in five second intervals for one minute to obtain a homogenous surface for generating demineralized and remineralized lesions. The samples were then imbedded in black orthodontic acrylic blocks. They were stored in tissues soaked in 1% Thymol solution and refrigerated to keep the hard tissue hydrated and to prevent bacterial growth.

2. Fiducial Marking

Two by two millimeter windows were cut on both the occlusal and buccal surfaces being studied with a TEA CO2 laser (Impact 2500, GSI Lumonics Rugby, UK). The fiducial markings extended into the enamel surface to a depth of 50 microns[19].

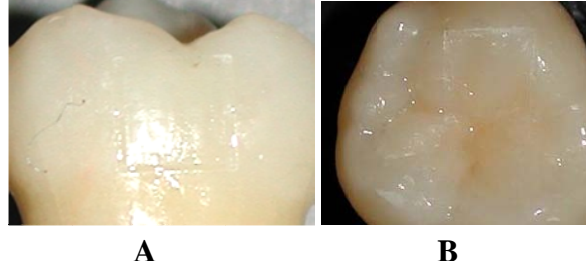


Figure 5. Fiducial markings on A) Buccal and B) Occlusal Surfaces

3. Enamel Varnish Application

The enamel outside of the 2X2 millimeter fiducial marking was painted using clear nail polish (Type, Revlon, City)[19]. Clear varnish is used in this study because it does not interfere with the imaging techniques. The area surrounding the 2X2 millimeter windows was painted to provide contrast between sound enamel and the enamel that would be subjected to demineralization and remineralization.

B. Demineralization Challenge

1. Demineralization

White spot lesions were created within the 2X2 windows using a demineralization regimen.

Each sample was placed into 50 ml of acetate buffer solution containing 2.0 mmol/L calcium, 2.0mmol/L phosphate, and 0.075mol/L acetate maintained at a pH 4.5 and a temperature of 37°. The samples were placed in solution for three 48 hour periods with the aliquot solution being changed out each period. The samples were then imaged using the following imaging techniques after each period[19].

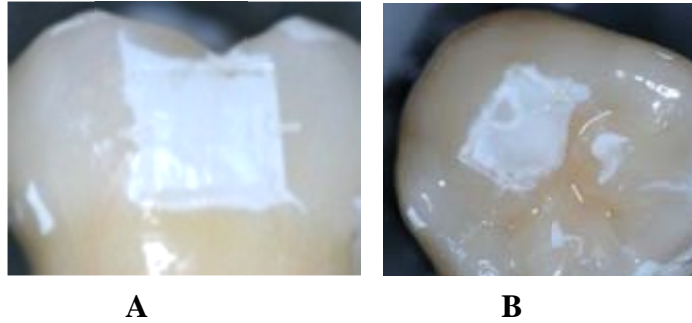


Figure 6. Demineralization A) Buccal and B) Occlusal Surfaces

2. Remineralization

The white spot lesions were then remineralized within the 2X2 windows using a solution at pH 7.0 containing 1.5mmol calcium as CaCl, 0.9mmol phosphate at KH₂PO₄ and 1ppm fluoride as NaF at 37°C[27].

The white spot lesions were remineralized using 50ml of the above solution. The samples were placed in the solution for two 92 hour periods. The samples were then imaged using the following imaging techniques after each period[19].

C. Methods of Imaging

1. Transillumination – NIR

The Transillumination - NIR imaging set-up for buccal lesions is shown previously in Figure 4. Light from a single-mode fiber-pigtail coupled to a 1310-nm superluminescent diode (SLD) with an output power of 15-mW and a 30-nm bandwidth, Model SLED1300D20A (Optospeed, Zurich, Switzerland), was connected to a 20-mm

NIR fibercollimator (Micro Laser Systems, Garden, Grove, CA). Crossed NIR polarizers, Model K46-252 (Edmund Scientific, Barrington, NJ), were used to remove light that directly illuminated the array without passing through the tooth. An InGaAs focal plane array (318x252 pixels), the Alpha NIR (Indigo Systems, Goleta, Ca) with an Infinimite lens (Infinity, Boulder, Co), was used to acquire all the images. The acquired 12 bit digital images were analyzed using IRVista software (Indigo systems, Goleta, CA). The illuminating light intensity, source to sample distance, and aperture diameter were adjusted for each sample to obtain the maximum contrast between the lesion and sound enamel without saturation of the InGaAs FPA around the lesion area. An example of an image produced by this method is shown in Figure 4.

For occlusal images, the 20-mm collimated beam was focused by a 150-mm focal length cylindrical lens at a point just above the dentinal-enamel junction, as shown in Figure 6. This configuration was found to reflect a fairly uniform intensity level across the occlusal plane[23]

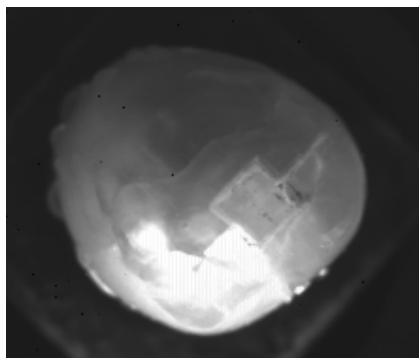


Figure 7. Transillumination Occlusal Surface

2. Reflected Light – NIR with Polarization

Polarized Reflected light – NIR images were taken with the same light sources, as shown in Figure 8. The near-infrared light was shined directly at the tooth, and reflected light coming out of the tooth was measured (Figure 8a). For occlusal images, the tooth was turned on its side so the light was incident on the occlusal surface (Figure 8b). The illuminating light intensity, source to sample distance, and aperture diameter were adjusted for each sample to obtain the maximum contrast between the lesion and sound enamel without saturation of the InGaAs FPA around the lesion area. An example of images obtained with NIR reflective with polarization is shown previously in Figure 3.

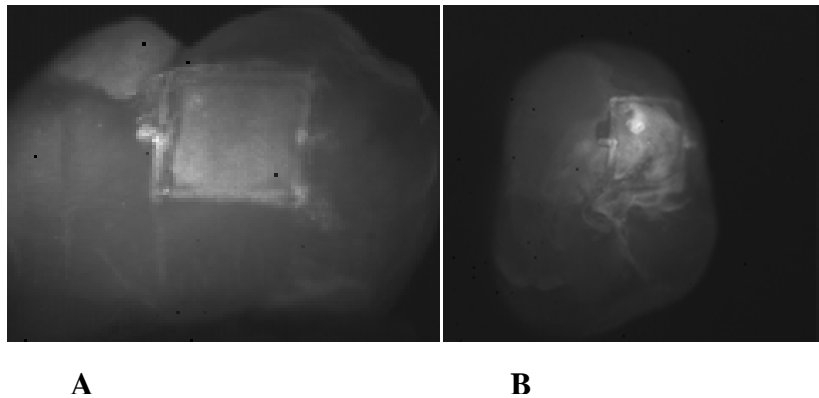


Figure 8. Reflectance A) Buccal and B) Occlusal Surface

3. Qualitative Light Fluorescence

Enamel surfaces were irradiated with a frequency doubled diode pumped solid state Nd:YVO₄ laser ($\lambda=473\text{-nm}$; DPSS Laser Model BLM-50; Extreme Lasers, Houston Texas) with an incident intensity of up to 50-mW. A 500-nm long-pass filter (LP-500) and a DFK 31AF03 FireWire camera (resolution 1024 x 768) from the Imaging Source (Charlotte, NC) were used to image the fluorescence from the surface. Imaging was

carried out in the dark to avoid the interference of ambient light. Figure 9 shows an example of images taken with QLF.

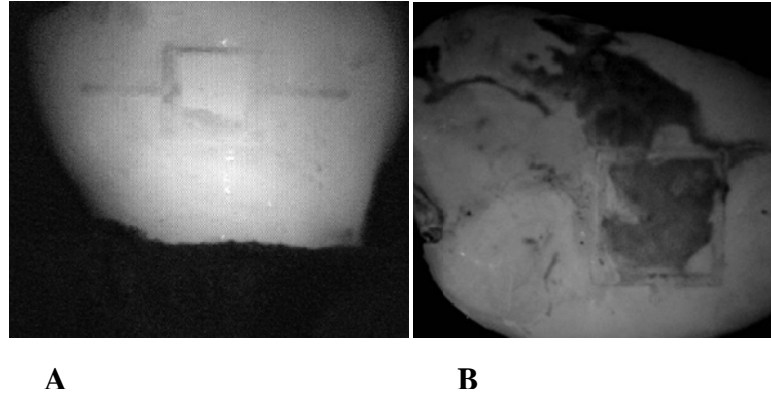


Figure 9. QLF A) Buccal and B) Occlusal Surface

4. Reflected Light- Visible with Polarization

In order to acquire reflected light images, visible or NIR, light was shined directly at the buccal or occlusal surface of the tooth and reflected light coming out of the tooth surface was imaged. Crossed polarizers were placed after the light source and before the detector. For occlusal images, the tooth was turned on its side so the light was incident on the occlusal surface. In this method, the demineralized region appears lighter than the sound enamel because the demineralized region scatters the light increasing the amount of light scattered/reflected back towards the camera. In order to acquire visible light images a tungsten halogen light source was used with a color firewire CCD camera with a resolution of 450 lines, (Model DFK 5002/N, Imaging Source), equipped with the same

Infinite lens used for NIR imaging. The NIR reflectance images were acquired using the same InGaAs FPA, NIR light source and polarizers used for the NIR transillumination measurements, however they were placed in a different orientation for reflectance measurements, that is, positioned to view or illuminate the same surface of the tooth[24].

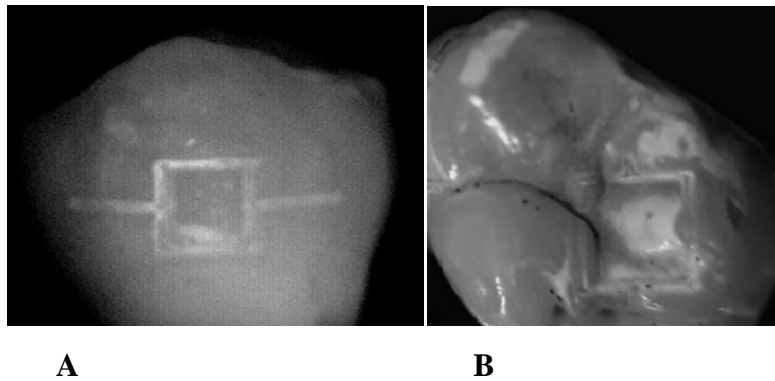


Figure 10. Visible A) Buccal and B) Occlusal Surface

D. Method of Image Analysis

NIR, QLF, and Visible Images were analyzed using the Igorpro software (Wavemetrics, Lake Oswego, OR). A line profile was taken as shown in Figure 11. Using the IgorPro software, a graph of the line out was generated.

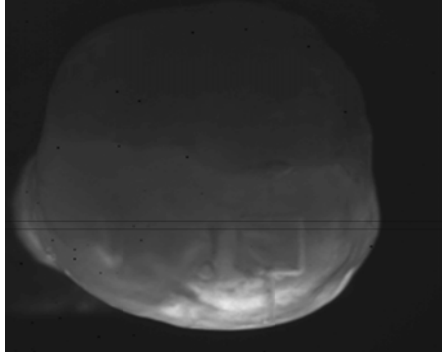


Figure 11. Line Profile

PS-OCT

1. PS-OCT Imaging

An all single-mode fiber autocorrelator-based Optical Coherence Domain Reflectometry system (OCDR; Optiphase, Inc., Van Nuys, CA) was used for PS-OCT imaging and is well described in previous studies.[25, 26]. This system used a polarization switching probe, high efficiency piezoelectric fiber-stretchers, and an InGaAs receiver.

The OCDR was integrated with a broadband high power superluminescent diode (SLD) (Denselight, Jessup, MD) with an output power of 45 mW and a bandwidth of 35-nm and a high-speed XY-scanning system (ESP 300 controller & 850HS stages, National Instruments, Austin, TX) for *in vitro* optical tomography. The probe was designed to provide a spot diameter of 50- μ m over a range of 10-nm.

Eight hundred scans were taken in the x-axis at 20 μ m intervals, and 3 scans in the y-axis at a distance of 150- μ m. The scans were taken across the whole 2X2 window, where the area of interest lies.

2. PS-OCT Line Profiles

In a perpendicular-axis PS-OCT image, the demineralized regions can be analyzed due to the backscatter created. In each sample, two line profiles were taken: one in the demineralized region, and one in the sound region. The position of the line profile was taken at the center of the lesion, or the center of the sound enamel (Figure 12).

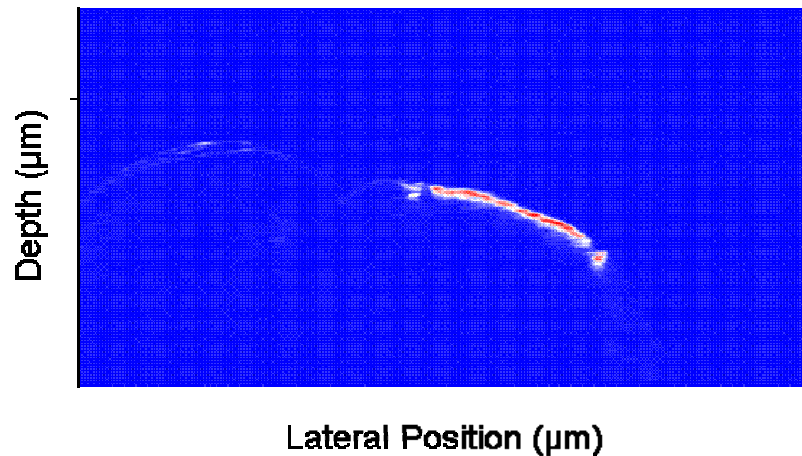


Figure 12. PS-OCT Line Profile taken through demineralized region

The data collected was then analyzed using a one-way analysis of variance (repeated measures ANOVA) was used followed by the Tukey-Kramer post-hoc multiple comparison test. The samples from the different periods were compared using the same imaging technique. The initial time point(T0), final demineralization(D4) and final remineralization(R4) from the different imaging techniques were then compared to one-another respectively.

Results

A. Buccal Images

Image contrasts for the buccal sample lesions were obtained using the IgorPro software program. The following tables and graphs show the contrast lesions using the different imaging techniques. The larger numbers show a greater contrast between demineralized and sound tooth structure. T0 indicates the initial time point. The “D” indicates Demineralization and the “R” indicates Remineralization. The number following specifies the cycle of demineralization or remineralization respectively.

The following figure shows the mean and standard deviations using Near-Infrared reflectance to measure the difference between the demineralized/sound and remineralized/sound tooth structure for each of the time points measured. There is a trend showing an increase in contrast as the demineralizing time points progress but a decrease in contrast during the remineralizing time points. The remineralizing contrast never reaches baseline at T0. The highest contrast is obtained at the final demineralization D4 time point with a .28 value.

NIR Reflectance Buccal

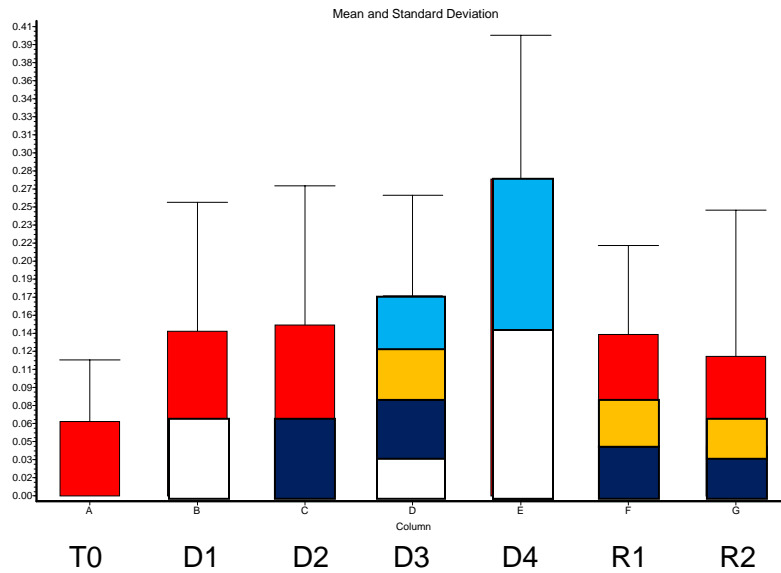


Figure 13. Comparison of NIR Reflectance Time Points Buccal. The error bars show standard deviation. Bars with the same colors are not significantly different from each other $p < .05$.

NIR Transillumination Buccal

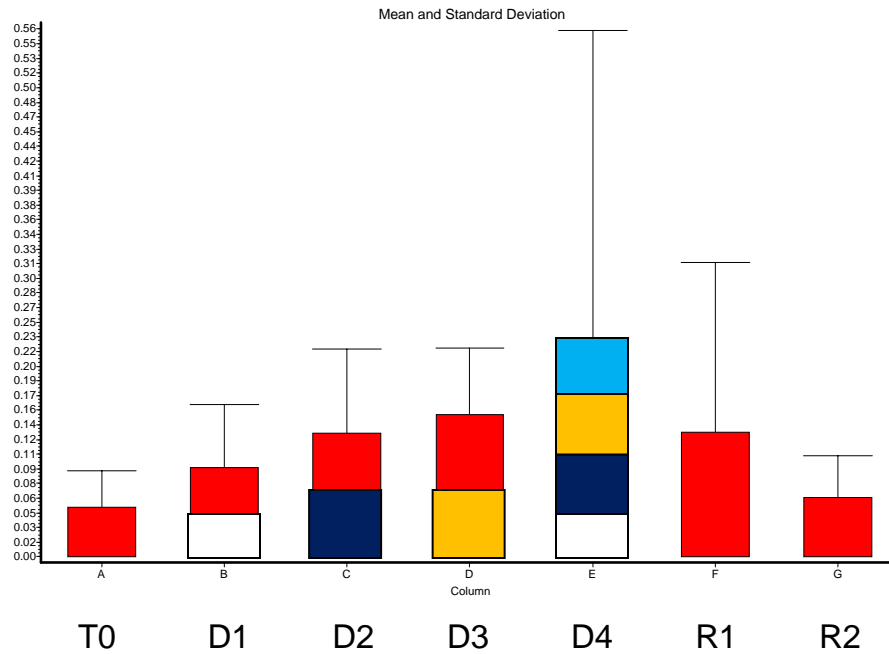


Figure 14. Comparison of NIR Transillumination Time Points. The error bars show standard deviation. Bars with the same colors are not significantly different from each other $p < .05$.

The values for the Near-Infrared transillumination technique also show an increase in contrast value as the demineralization time points progress and a decrease in value at the remineralization time points. The highest value at .23 is at the final demineralization time point D5.

QLF Buccal

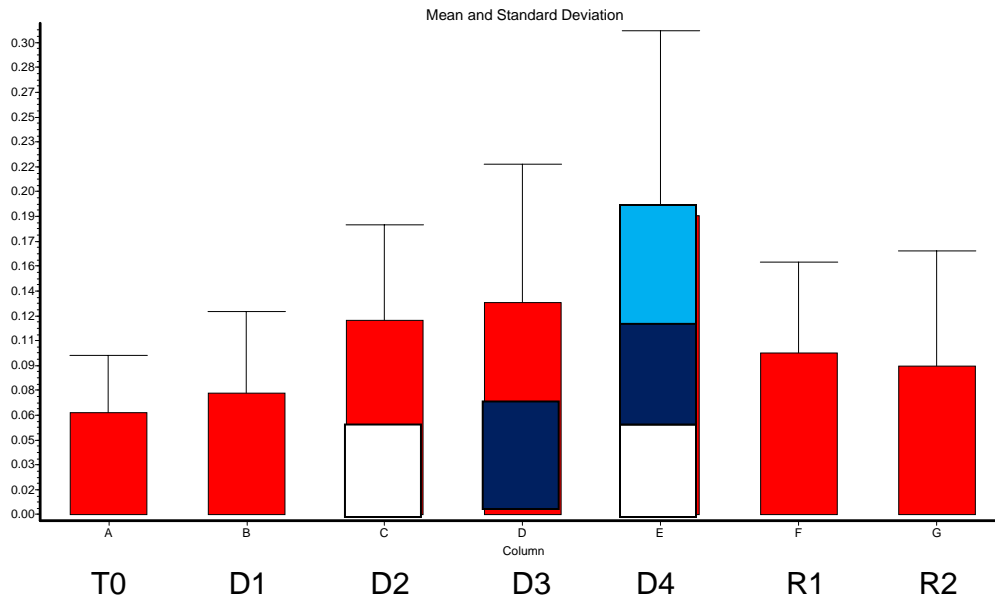


Figure 15. Comparison of QLF Time Points. The error bars show standard deviation. Bars with the same colors are not significantly different from each other $p < .05$.

The images obtained with the Quantitative Light Fluorescence technique shows a similar trend as the above two techniques. The highest value obtained is .19 at the final demineralization time point.

Visible Buccal

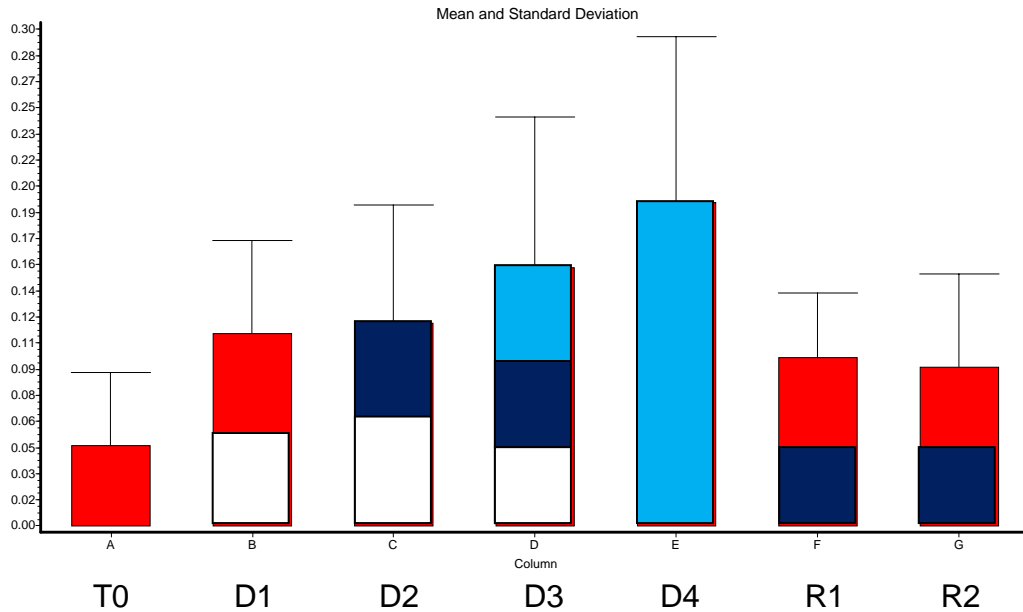


Figure 16. Comparison of Visible Light Time Points. The error bars show standard deviation. Bars with the same colors are not significantly different from each other $p < .05$.

The images from the visible imaging technique also show an increase in contrast as the demineralization cycles progress and a subsequent decrease in contrast as the remineralizing cycles begin. The values never reach baseline. The trend is similar to the above techniques.

TO Buccal

Groups	Mean	SD
Quantitative Light Fluorescence	0.06417	0.03577
Visible	0.04826	0.04327
NIR Reflectance	0.06511	0.05286
NIR Transillumination	0.05326	0.0384

Table 1 Comparison T0 Buccal

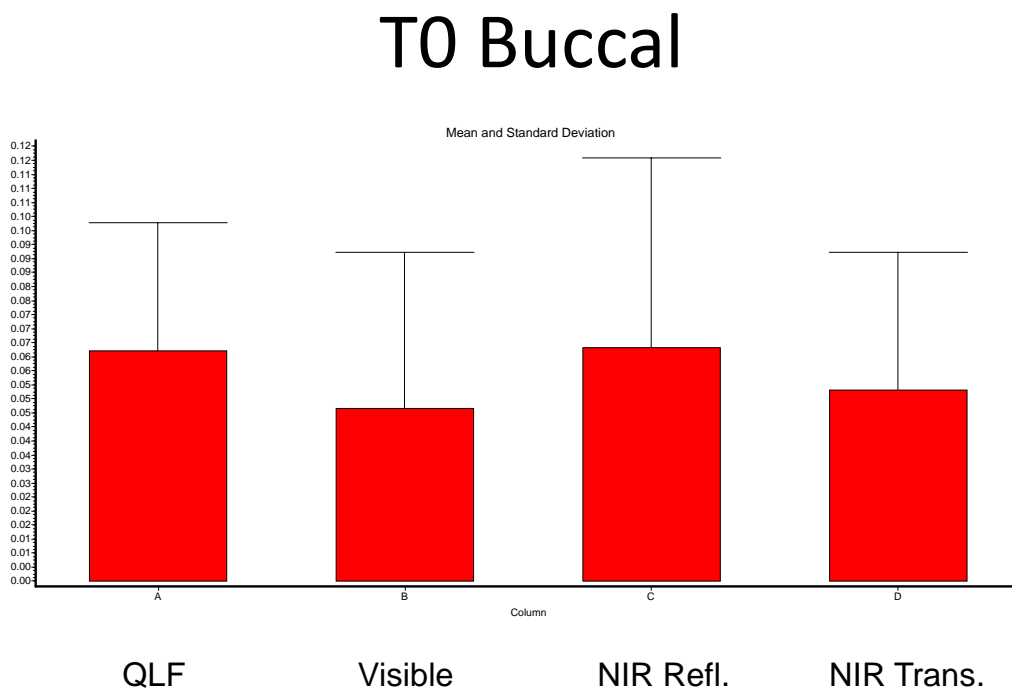


Figure 17. Comparison of T0 Buccal Surface

A one-way analysis of variance (repeated measures ANOVA) was used followed by the Tukey-Kramer post-hoc multiple comparison test was used to analyze the data.

The contrast values of the four groups compared at time point zero shows that NIR reflectance shows the highest contrast values at .07. The P values are listed in the following table. The groups did not break in statistical significance from one another.

D4 Buccal

Groups	Mean	SD
Quantitative Light Fluorescence	0.1882	0.116
Visible	0.1936	0.09877
NIR Reflectance	0.2751	0.1242
NIR Transillumination	0.2321	0.3288

Table 2 Comparison D4 Buccal

Final Demineralization Buccal

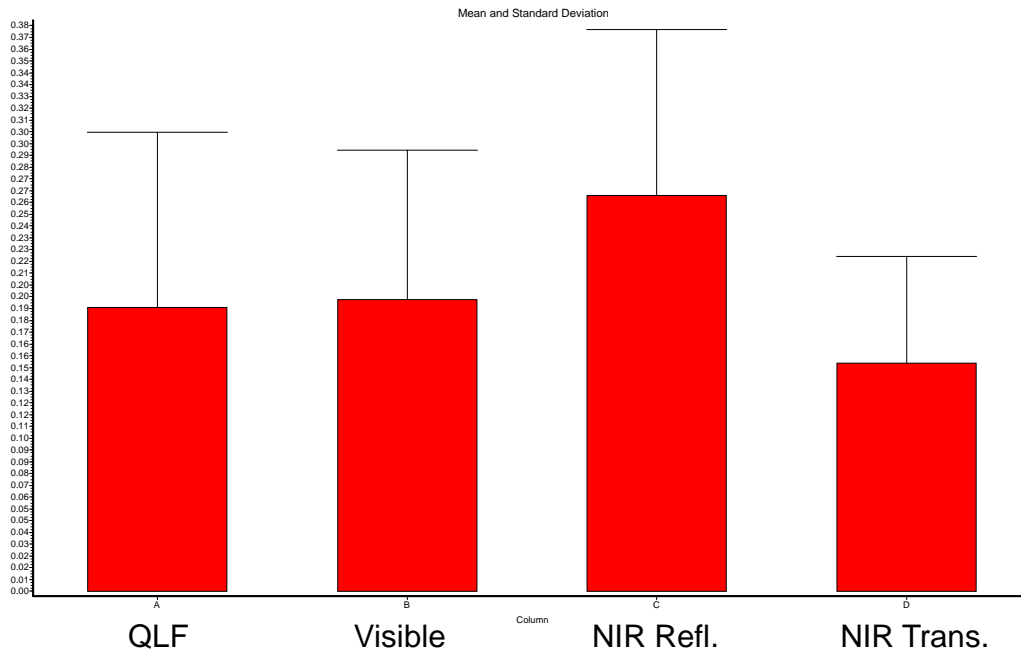


Figure 18. Comparison of D4 Buccal Surface

The groups compared at the final demineralization time point shows that NIR reflectance has the highest contrast value at .28. The P values are shown in the following table. The groups did not show statistical difference when comparing the means.

R2 Buccal

Groups	Mean	SD
Quantitative Light Fluorescence	0.09374	0.07226
Visible	0.09533	0.05545
NIR Reflectance	0.1214	0.1262
NIR Transillumination	0.06351	0.04374

Table 3 Comparison R2 Buccal

Final Remineralization Buccal

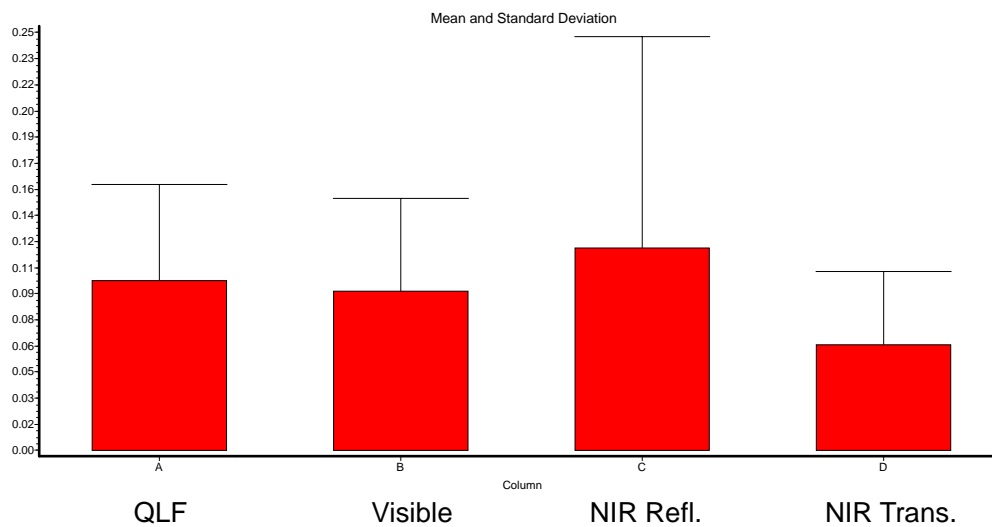


Figure 19. Comparison of R2 Buccal Surface

A similar trend was observed during the final remineralizing time point with NIR Reflectance at the highest contrast value of .12. The following table shows the P values. There was no statistical difference between the four groups.

Buccal OCT	Column1	Column2
Sample	Lesion	Sound
1	1967.11	587.16
2	1711.64	731.438
3	1077.65	140.7
4	1288.12	208.68
5	341.786	66.09
6	317.907	85.1413
7	814.064	242.761
8	1221.8	276.56
9	492.21	50.47
10	787.535	92.15
11	891.824	201.59
12	339.943	474.66
13	707.595	263.89
14	1482.37	456.57
15	2720	530.027
16	1654.31	397.96

Table 4 OCT Values Buccal

OCT results are depicted in table 8. These values show that there is significant demineralization in all the buccal lesions.

B. Occlusal Images

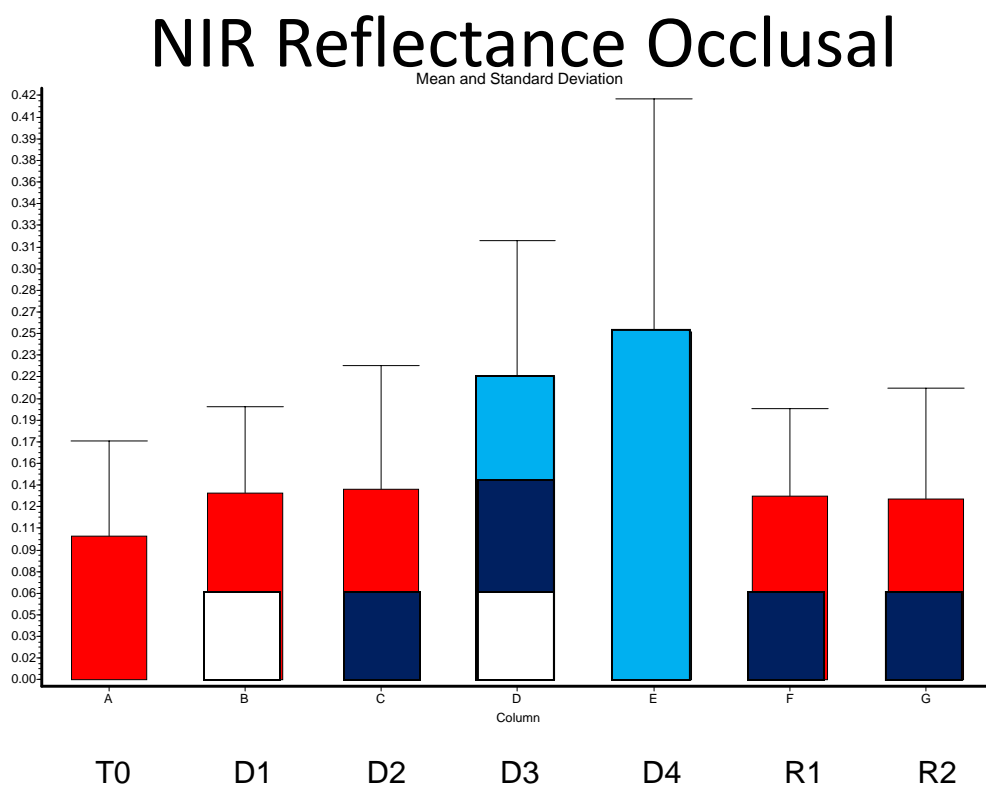


Figure 20. Comparison of NIR Reflectance Time Points. The error bars show standard deviation. Bars with the same colors are not significantly different from each other $p < .05$.

There is an increase in contrast during the demineralization cycles followed by a decrease in contrast during the remineralization cycles.

QLF Occlusal

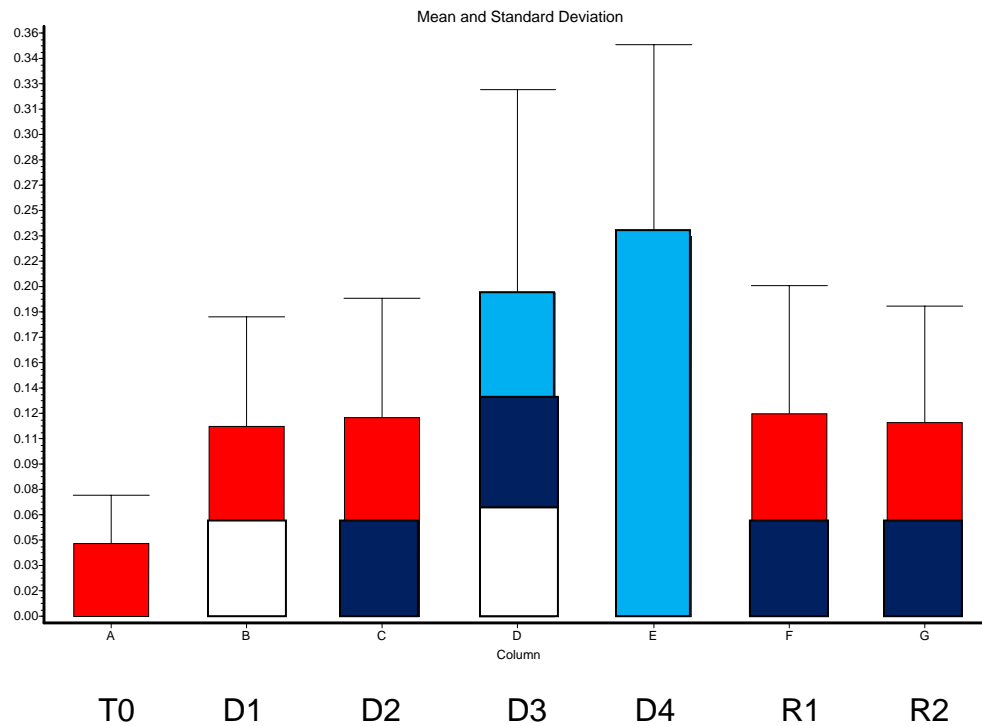


Figure 21. Comparison of QLF Time Points. The error bars show standard deviation. Bars with the same colors are not significantly different from each other $p < .05$.

There is an increase in contrast during the demineralization cycles with the highest value obtained at D4 .23. R1 and R2 both show a decrease in contrast compared to the D4.

Visible Occlusal

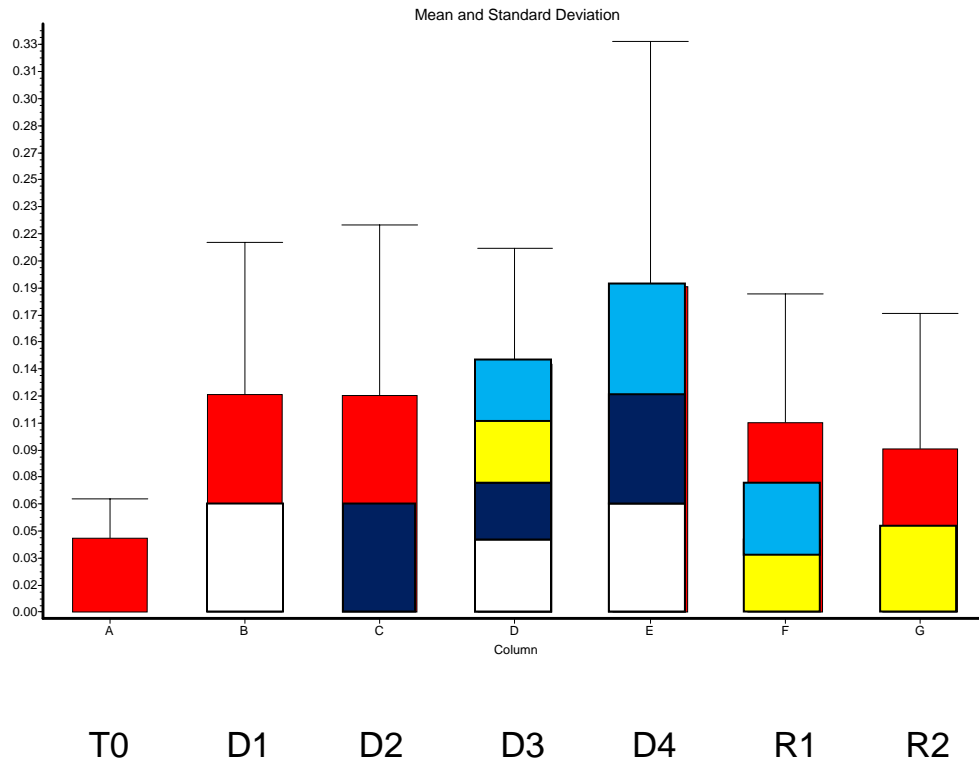


Figure 22. Comparison of Visible Light Time Points. The error bars show standard deviation. Bars with the same colors are not significantly different from each other $p < .05$.

The trend observed in the visible occlusal similar to the other imaging techniques. An increase in contrast during demineralization followed by a decrease in contrast during the remineralization cycles.

TO Occlusal

Groups	Mean	SD
Quantitative Light Fluorescence	0.04536	0.0297
Visible	0.04323	0.02246
NIR Reflectance	0.104	0.06822

Table 5 Comparison T0 Occlusal Surfaces

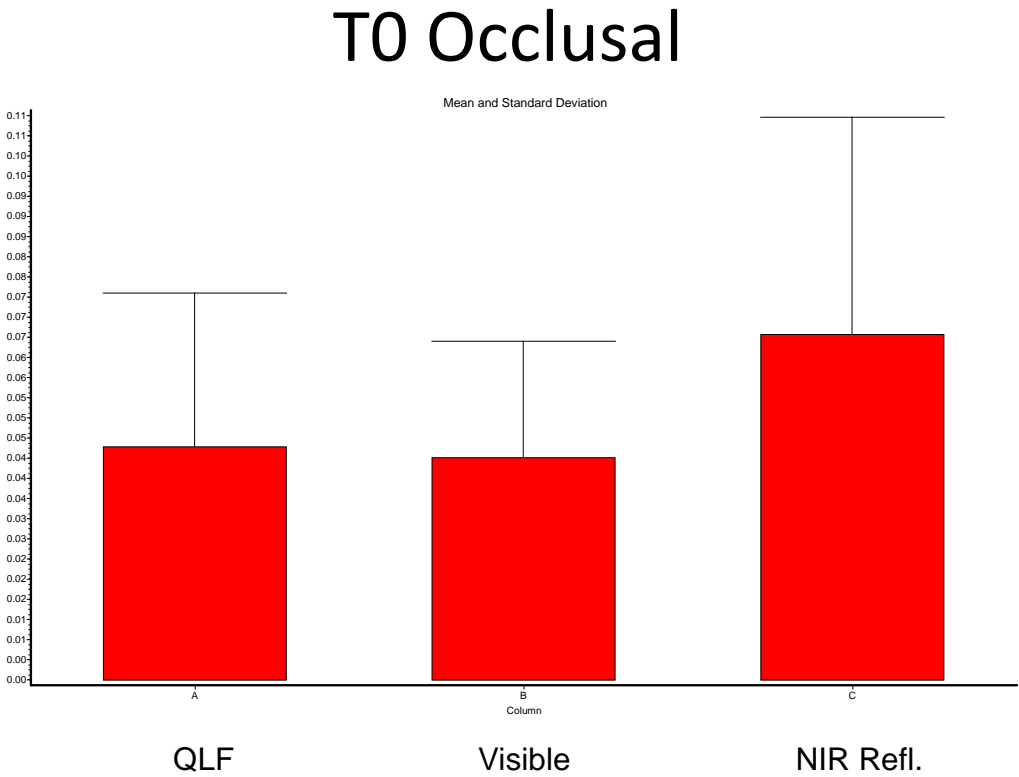


Figure 23. Comparison of T0 Occlusal Surface

The three groups did not show statistical difference at T0.

D4 Occlusal

Groups	Mean	SD
Quantitative Light Fluorescence	0.2348	0.1178
Visible	0.1884	0.1416
NIR Reflectance	0.2517	0.1679

Table 6 Comparison D4 Occlusal Surfaces

Final Demineralization Occlusal

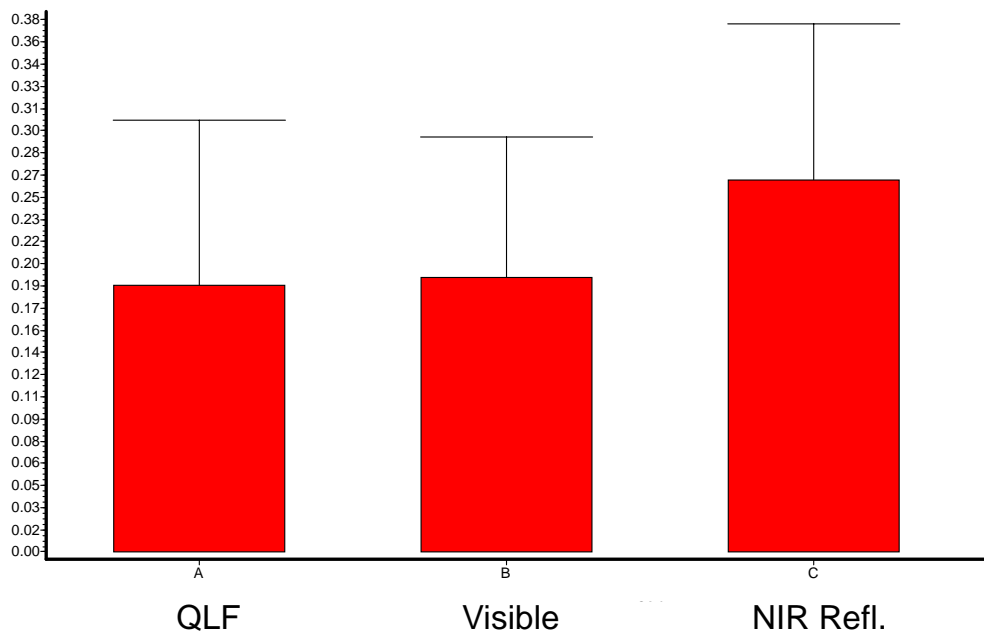


Figure 24. Comparison of D4 Occlusal Surface

Statistical difference was not shown during the final demineralization cycle. NIR reflectance did however show the highest contrast value when compared to QLF and Visible.

R2 Occlusal		
Groups	Mean	SD
Quantitative Light Fluorescence	0.1197	0.0718
Visible	0.09442	0.07843
NIR Reflectance	0.1312	0.07959

Table 7 Comparison R2 Occlusal Surfaces

Final Remineralization

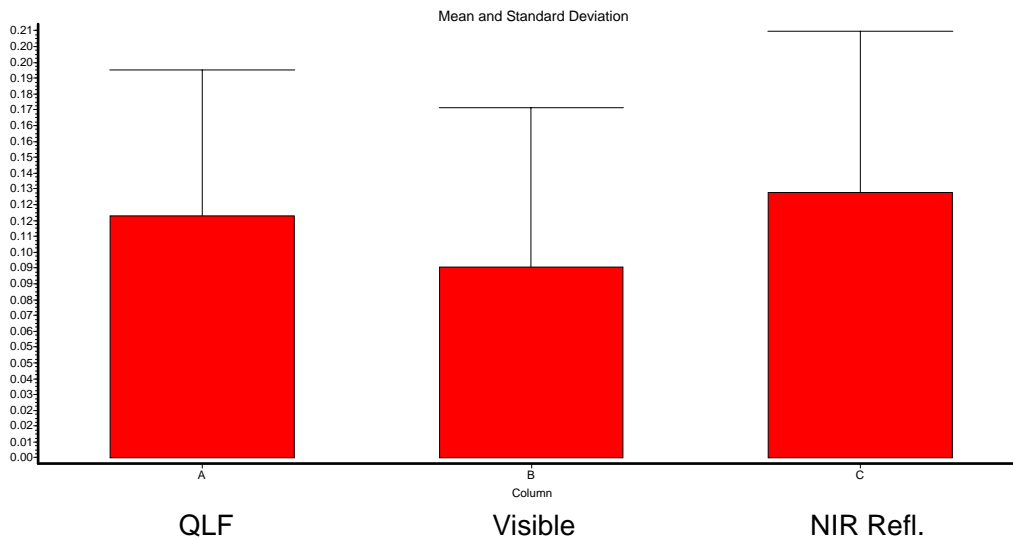


Figure 25. Comparison of R2 Occlusal Surface

Statistical difference was not shown during the final remineralization cycle. NIR reflectance showed the highest contrast value when compared to QLF and Visible.

Occlusal	Lesion	Sound
1	336.851	109.93
2	619.795	134.557
3	988.216	192.554
4	1062.77	182.145
5	222.138	147.655
6	1374.11	188.233
7	1031.39	157.38
8	1150.32	150.924
9	607.185	98.7056
10	225.747	68.67
11	552.177	93.55
12	710.153	102.608
13	915.202	88.59
14	491.3	161.3
15	1145.14	58.43
16	514.21	143.94

Table 8 OCT Values Occlusal

OCT results are depicted in Table 15. These values show that there is significant demineralization in all the Occlusal lesions.

Discussion

The purpose this study was to determine if high contrast images could be obtained between sound and artificially demineralized and remineralized lesions in enamel using NIR imaging and other imaging modalities such as Quantitative Light Fluorescence and Visible Imaging with Cross-Polarization. We also wanted to test if NIR provided greater contrast in the images than the other imaging modalities. Both buccal surface and occlusal surfaces were measured in this study.

The results show that all of the imaging modalities depicted an increase in contrast in the lesions as the demineralization cycles progressed. In comparing the different imaging modalities at the same time point we see that NIR reflectance offers the highest contrast between the groups but the numbers did not break significantly from the other groups. There was wide overlap between the standard deviations in the different groups. The trend was observed in both the buccal and occlusal surfaces.

The remineralization cycle we see a decrease in the contrast value from the demineralization values and they never reach the initial contrast values at T0. When comparing the imaging modalities at the remineralization cycles we see that NIR again offers the highest contrast values with a subsequent decrease in contrast imaging as the remineralization cycles progressed. There was also no statistical significant break between the groups and there was a large overlap in standard deviation in the groups. The trend was observed in both the buccal and occlusal surfaces.

The highest contrast was obtained using NIR reflectance at 1310nm and the measurements are similar to QLF imaging measurements. This study shows that all of the modalities used are effective at early white spot lesion detection in enamel.

The sample size used in this study was relatively small and may account for the different groups not acquiring statistical significance. Similar trends have been reported in similar studies with NIR offering the highest contrast between sound and demineralized enamel. A larger sample size may aid in obtaining clear differences between groups.

All imaging methods are angle sensitive. The direction at which the probe is aimed at the tooth changes the image greatly. It is possible that in this study the greatest image contrast was not achieved due to the sample position in relationship to the probe. Care was taken to move the sample and to focus the probe so the best image was achieved but ultimately only one image was taken for each sample for each imaging modality.

This study used clear varnish to prevent demineralization as established by previous studies by Fried et al. The varnish has been shown to be effective at preventing demineralization. It provides a barrier against the demineralization and remineralization solutions that are used in the study. It is however difficult to tell if the varnish has been applied uniformly to the tooth surface or if the varnish has flown into the fiducial box or into the occlusal grooves of the samples. Over time the varnish cracks and chips off the surface making the demineralized /remineralized regions difficult to identify. Many of the samples showed uneven lesion formation within the fiducial box, this could have been

due to the varnish flowing into the fiducial box or incorrect application. In the future a better method for applying the varnish and extra care to prevent any varnish in the study areas should be developed.

When determining where to take the line profile for the samples it was decided that the bottom half of the fiducial mark would be measured. This was our attempt to keep the measurements as uniform as possible for all of the readings. The samples were measured using many methods with different time points and our method for standardizing the measurements was taking the line profile at the bottom half of the fiducial box. Future studies should take multiple line profiles throughout the fiducial box to determine the extent of demineralization/remineralization. The results can then be averaged to account for any variation.

Early studies have shown that fluorosis, staining and pigmentation do not affect imaging demineralization with NIR. Thus NIR eliminates confounding variables that may interfere with visible diagnosis of dental decay and demineralization. False positives are can also be prevented using this imaging technique, [25]. This is a big advantage that NIR has over QLF imaging. QLF does not determine between staining and fluorosis. Light scattering in sound enamel is weak with NIR and increases as enamel is demineralized. This is the advantage that NIR has over Visible with polarization because scattering of light in sound enamel is high with Visible imaging.

QLF has not been shown in previous studies to be effective on occlusal lesions. It did not perform as well in our study. QLF has been shown to be a promising imaging technique for early detection of demineralization. A big draw back to the technique is

that the imaging has to be done in the dark due to the effect ambient light on the measurements. Extraneous light affects the measurements and decreases the contrast readings. QLF is also not good at detection of subsurface lesions and is not as effective at detection of orthodontic white spot lesions due to the size and pattern of demineralization around the orthodontic bracket. It would be difficult to capture a QLF image with optimal light intensity in any part of the lesion[27].

Previous studies have shown that PS-OCT correlates with the gold standard of microradiography and with polarized light microscopy. We used PS-OCT in this study to show the depth of demineralized lesion. The results show that lesions were present in the areas of demineralization.

Future studies are needed to determine if NIR is effective at determining demineralization/remineralization *in vivo*. These imaging techniques can be useful in the orthodontic profession, with quantitative identification of enamel being more valuable than qualitative and subjective analysis of demineralization obtained with visual inspection. More work is needed to develop this technology and to make it more compatible with clinical work.

Conclusion

This study suggests that NIR imaging offers higher contrast than the other imaging techniques. There is also a clear trend in contrast values during the demineralization cycles and the remineralization cycles. This study shows that NIR imaging with cross polarization is a promising tool to aid clinicians in qualifying demineralization and white

spots in enamel. Another advantage is that it aids clinicians in treatment of white spot lesions in the early stages before there is significant change in enamel appearance or before surgical intervention is needed. Non-surgical intervention can be appropriately implemented with useful treatments such as fluoride, chlorhexidine and behavioral modification.

NIR is a safe non-destructive imaging technique and multiple images can be acquired during treatment to determine if preventative therapy is effective or if more aggressive therapy needs to be prescribed. The lesion can be monitored through treatment to determine if it is expanding or arrested. Thus, NIR is a promising tool to be used in clinical treatment.

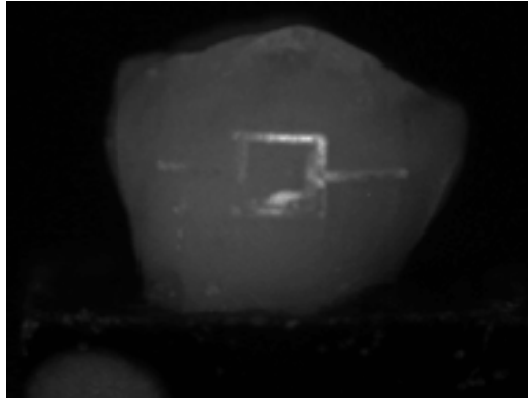
References

1. Murdoch-Kinch, C.A. and M.E. McLean, *Minimally invasive dentistry*. J Am Dent Assoc, 2003. **134**(1): p. 87-95.
2. Zero, D.T., et al., *The biology, prevention, diagnosis and treatment of dental caries: scientific advances in the United States*. J Am Dent Assoc, 2009. **140 Suppl 1**: p. 25S-34S.
3. Aljehani, A., et al., *In vitro quantification of white spot enamel lesions adjacent to fixed orthodontic appliances using quantitative light-induced fluorescence and DIAGNOdent*. Acta Odontol Scand, 2004. **62**(6): p. 313-8.
4. Jones, R.S. and D. Fried, *Remineralization of enamel caries can decrease optical reflectivity*. J Dent Res, 2006. **85**(9): p. 804-8.
5. Ogaard, B., et al., *Orthodontic appliances and enamel demineralization. Part 2. Prevention and treatment of lesions*. Am J Orthod Dentofacial Orthop, 1988. **94**(2): p. 123-8.
6. Svensater, G., et al., *The acid-tolerant microbiota associated with plaque from initial caries and healthy tooth surfaces*. Caries Res, 2003. **37**(6): p. 395-403.
7. Islam, B., S.N. Khan, and A.U. Khan, *Dental caries: from infection to prevention*. Med Sci Monit, 2007. **13**(11): p. RA196-203.
8. Coykendall, A.L., *Classification and Identification of the Viridans Streptococci*. Clinical Microbiology Reviews, 1989. **2**(3): p. 315-328.
9. Jefferson, K.K., *What drives bacteria to produce a biofilm?* FEMS Microbiol Lett, 2004. **236**(2): p. 163-73.
10. Featherstone, J.D., *Prevention and reversal of dental caries: role of low level fluoride*. Community Dent Oral Epidemiol, 1999. **27**(1): p. 31-40.
11. Marthaler, T.M., *Changes in the prevalence of dental caries: how much can be attributed to changes in diet?* Caries Res, 1990. **24 Suppl 1**: p. 3-15; discussion 16-25.
12. Travess, H., D. Roberts-Harry, and J. Sandy, *Orthodontics. Part 6: Risks in orthodontic treatment*. Br Dent J, 2004. **196**(2): p. 71-7.
13. Hu, W. and J.D. Featherstone, *Prevention of enamel demineralization: an in-vitro study using light-cured filled sealant*. Am J Orthod Dentofacial Orthop, 2005. **128**(5): p. 592-600; quiz 670.
14. Mitchell, L., *An investigation into the effect of a fluoride releasing adhesive on the prevalence of enamel surface changes associated with directly bonded orthodontic attachments*. Br J Orthod, 1992. **19**(3): p. 207-14.
15. Benson, P.E., N. Pender, and S.M. Higham, *Quantifying enamel demineralization from teeth with orthodontic brackets - a comparison of two methods. Part 1: repeatability and agreement*. European Journal of Orthodontics, 2003. **25**(2): p. 149-158.
16. Kanthathas, K., D.R. Willmot, and P.E. Benson, *Differentiation of developmental and post-orthodontic white lesions using image analysis*. Eur J Orthod, 2005. **27**(2): p. 167-72.
17. Willmot, D.R., et al., *Reproducibility of quantitative measurement of white enamel demineralisation by image analysis*. Caries Res, 2000. **34**(2): p. 175-81.

18. Wigdor, H.A., et al., *Lasers in dentistry*. Lasers Surg Med, 1995. **16**(2): p. 103-33.
19. Spitzer, D. and J.T. Bosch, *The absorption and scattering of light in bovine and human dental enamel*. Calcif Tissue Res, 1975. **17**(2): p. 129-37.
20. Lagerweij, M., et al., *The validity and repeatability of three light-induced fluorescence systems: An in vitro study*. Caries Res, 1999. **33**(3): p. 220-6.
21. Hirasuna, K., D. Fried, and C.L. Darling, *Near-infrared imaging of developmental defects in dental enamel*. J Biomed Opt, 2008. **13**(4): p. 044011.
22. Lee, C., C.L. Darling, and D. Fried, *Polarization-sensitive optical coherence tomographic imaging of artificial demineralization on exposed surfaces of tooth roots*. Dent Mater, 2009. **25**(6): p. 721-8.
23. Christopher M. Buhler, P.N.a.D.F., *Imaging of occlusal dental caries (decay) with near-IR light at 1310-nm*. Optical Express, 2005. **13**(2): p. 573-582.
24. Wu, J. and D. Fried, *High contrast near-infrared polarized reflectance images of demineralization on tooth buccal and occlusal surfaces at $\lambda = 1310\text{-nm}$* . Lasers Surg Med, 2009. **41**(3): p. 208-13.
25. Bush J, D.P., Marcus M. , *All-fiber optic coherence domain interferometric techniques*. SPIE, 2000: p. 71-80.
26. D. Fried, J.X., S. Shafi, J.D.B. Featherstone, T. Breunig, and C.Q. Lee, *Early detection of dental caries and lesion progression with polarization sensitive optical coherence tomography*. J Biomed Opt, 2002. **7**: p. 618-627.
27. Aljehani, A., et al., *In vivo reliability of an infrared fluorescence method for quantification of carious lesions in orthodontic patients*. Oral Health Prev Dent, 2006. **4**(2): p. 145-50.
25. Dowsett DJ, Kenny PA, Johnston RE. The physics of diagnostic imaging. NY: Chapman & Hall Medical 1998
26. Buhler CM, Ngaotheppitak P, Fried D. Imaging of occlusal dental caries (decay) with near-IR light at 1310-nm. Opt Expr 2005;13:573-582
27. Jones RS, Fried D. Remineralization of enamel caries can decrease optical reflectivity. J Dent Res 2006;85:804-808.
28. Chong SL, Darling CL, Fried D. Nondestructive measurement of the inhibition of demineralization on smooth surfaces using polarization-sensitive optical coherence tomography. Lasers Surg Med 2007;39:422-427.
29. Jones RS, Darling CL, Featherstone JDB, Fried D. Imaging artificial caries on occlusal surfaces with polarization sensitive optical coherence tomography. Caries Res 2004; 40:81-89.
30. Ngaotheppitak P, Darling CL, Fried D, Bush J, Bell S. PSOCT of occlusal and interproximal caries lesions viewed from occlusal surfaces, Lasers in Dentistry X, Vol. 6137. SPIE 2006: p 61370L.
31. Bush J, Davis P, Marcus MA. All-fiber optic coherence domain interferometric techniques, fiber optic sensor technology II, Vol. 4204. San Jose, TX, SPIE 2000: pp 71-80.

Appendix A: Buccal Surfaces

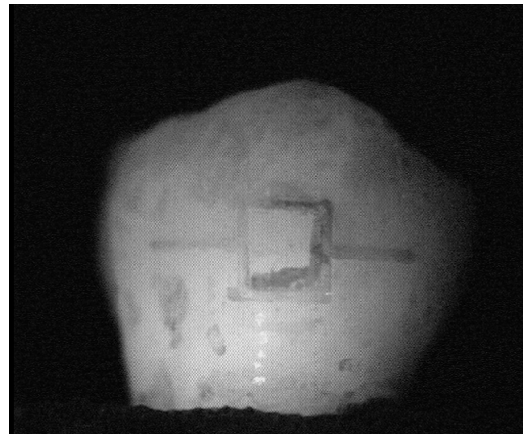
Sample 1



NIR Reflectance

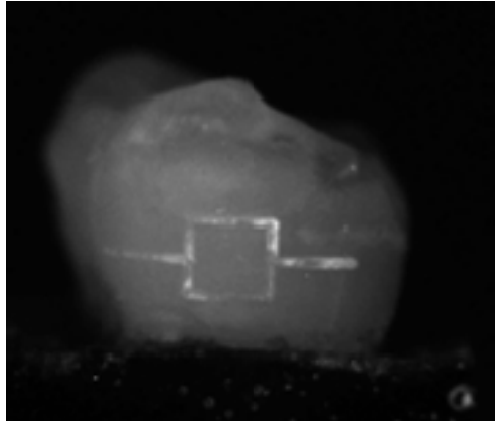


Visible



QLF

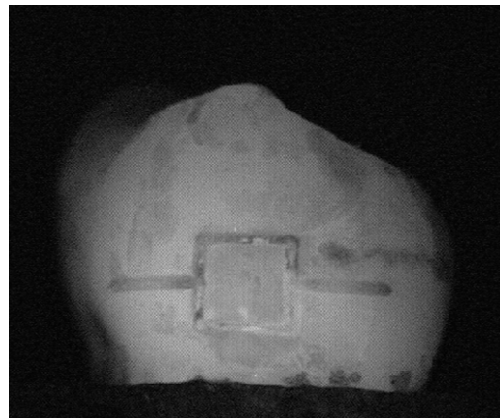
Sample 2



NIR Reflectance

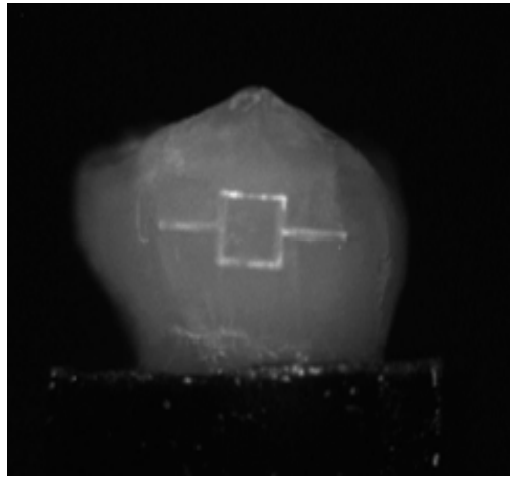


Visible



QLF

Sample 3



NIR Reflectance

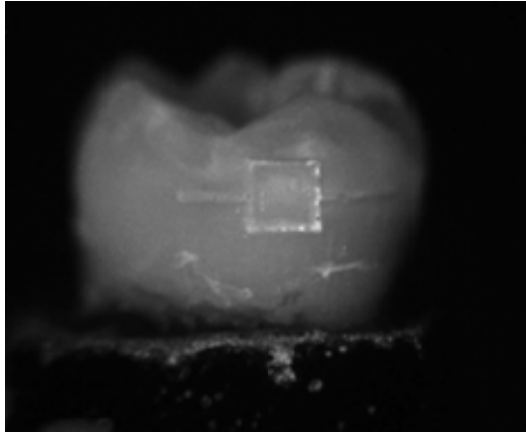


Visible



QLF

Sample 4



NIR Reflectance

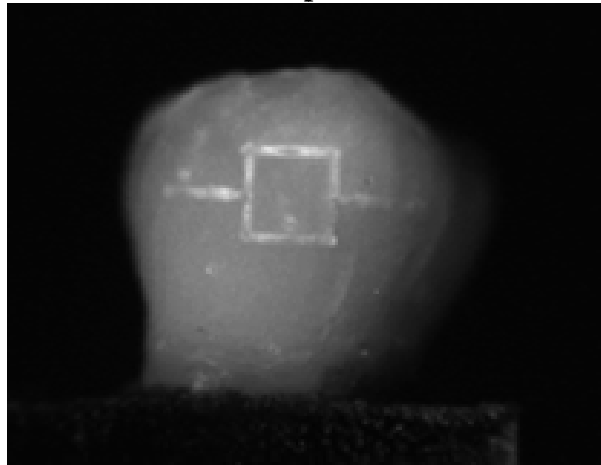


Visible



QLF

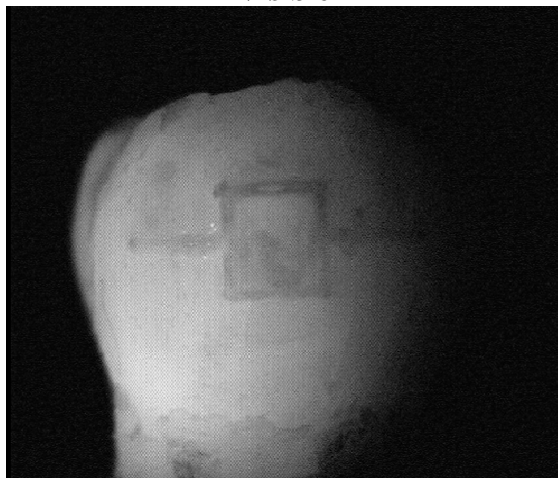
Sample 5



NIR Reflectance

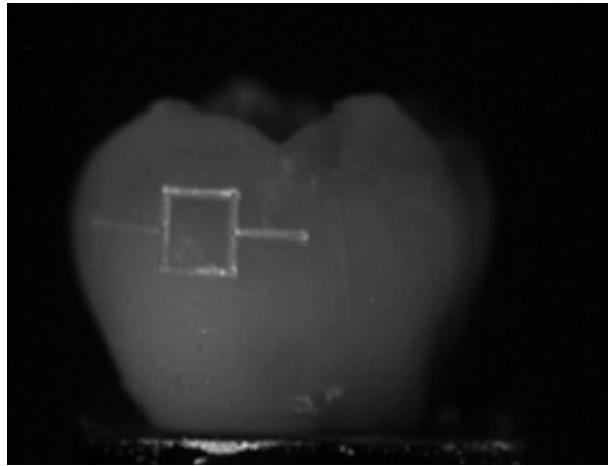


Visible



QLF

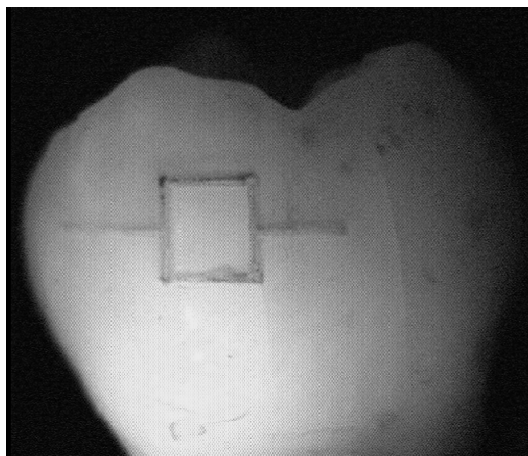
Sample 6



NIR Reflectance

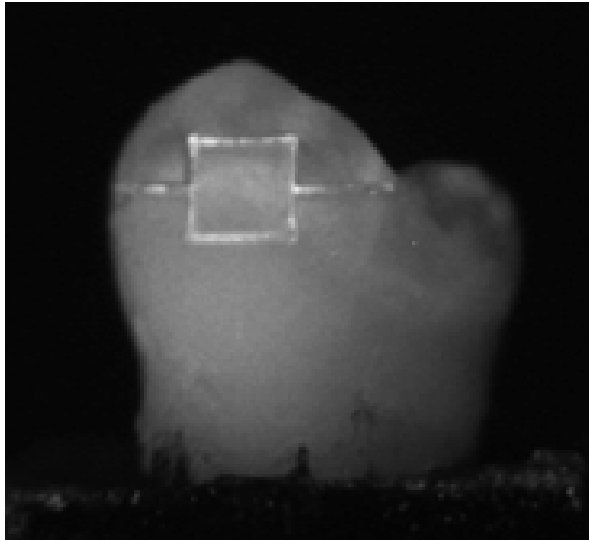


Visible



QLF

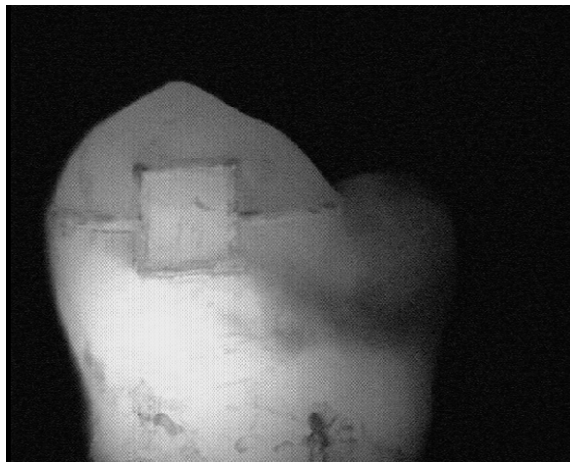
Sample 7



NIR Reflectance

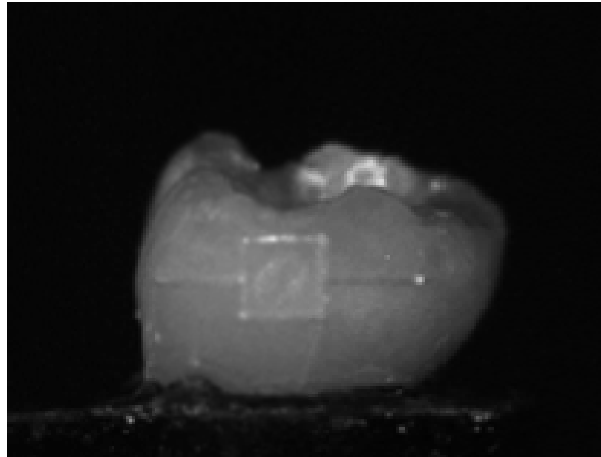


Visible

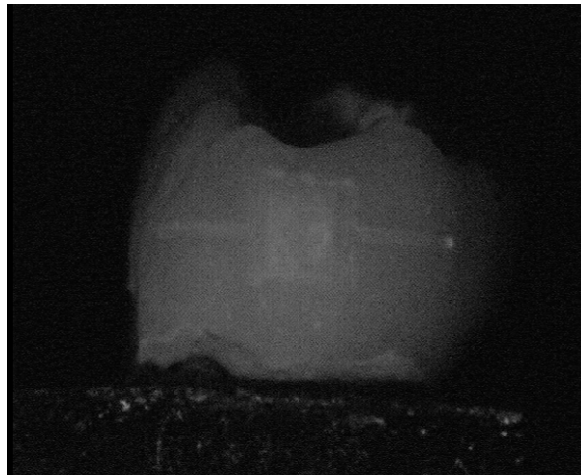


QLF

Sample 8



NIR Reflectance

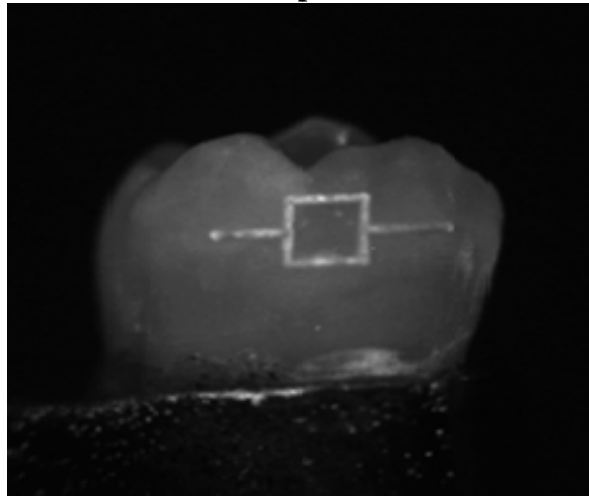


Visible



QLF

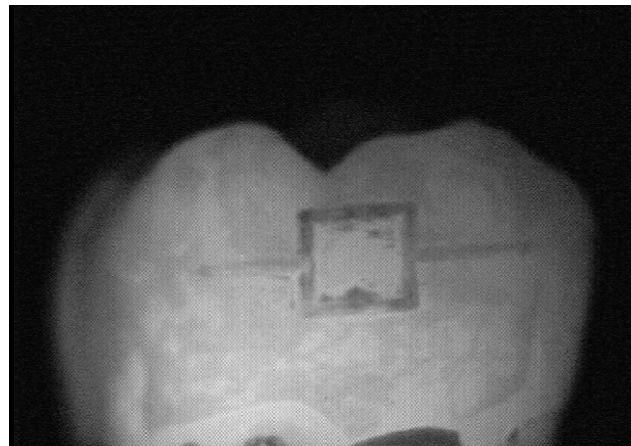
Sample 9



NIR Reflectance

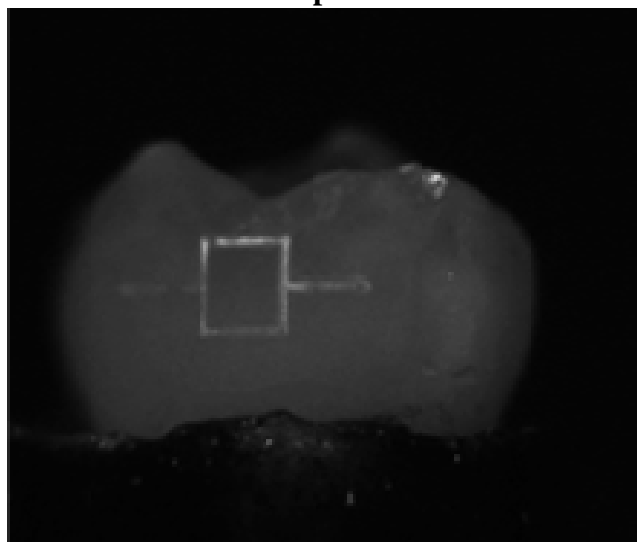


Visible



QLF

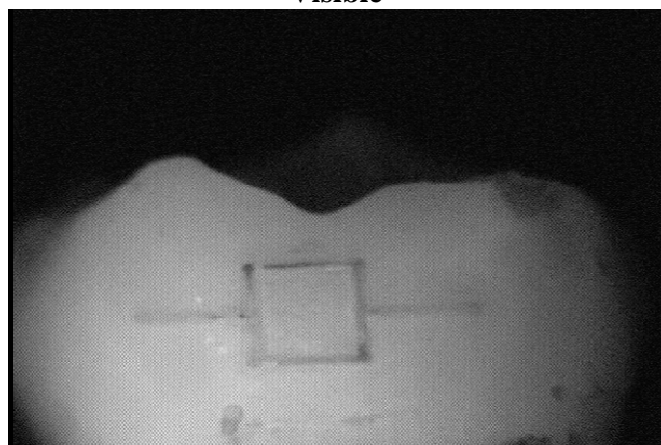
Sample 10



NIR Reflectance

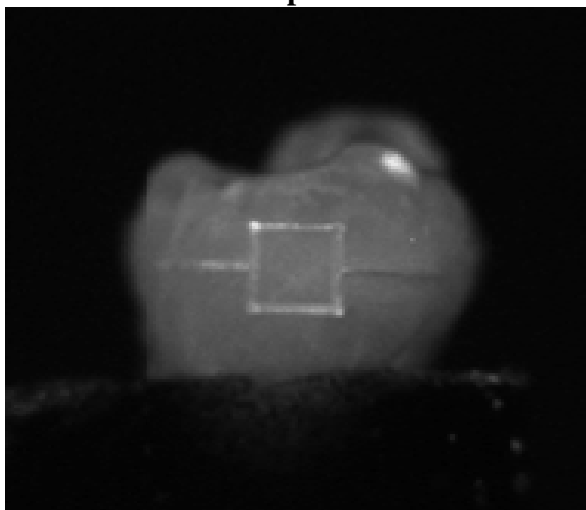


Visible



QLF

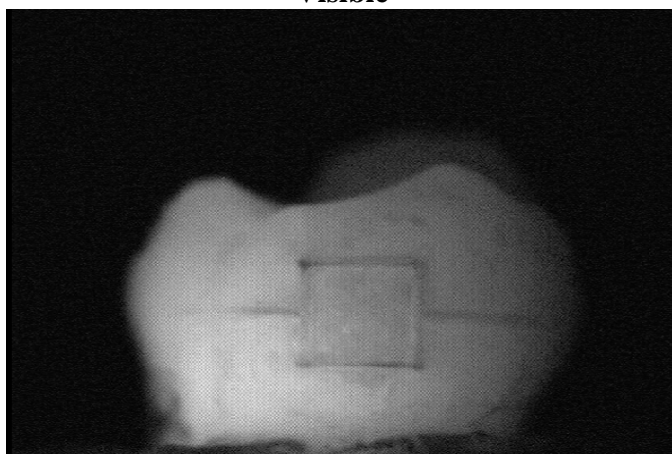
Sample 11



NIR Reflectance

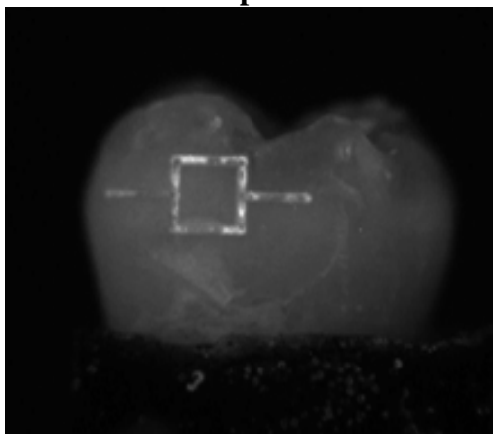


Visible



QLF

Sample 12



NIR Reflectance

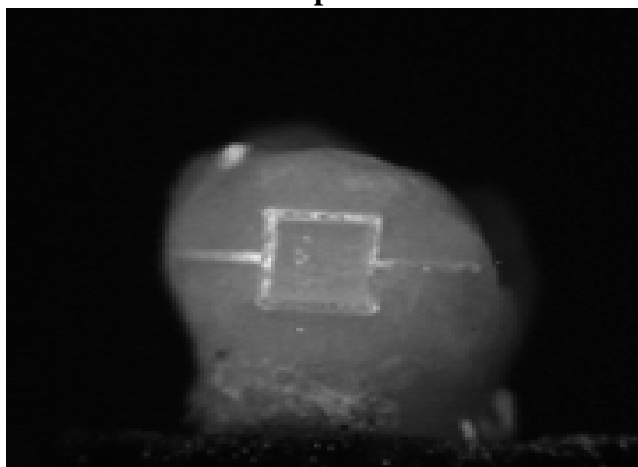


Visible

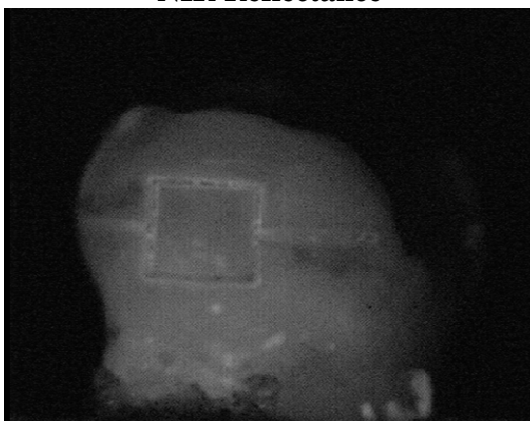


QLF

Sample 13



NIR Reflectance

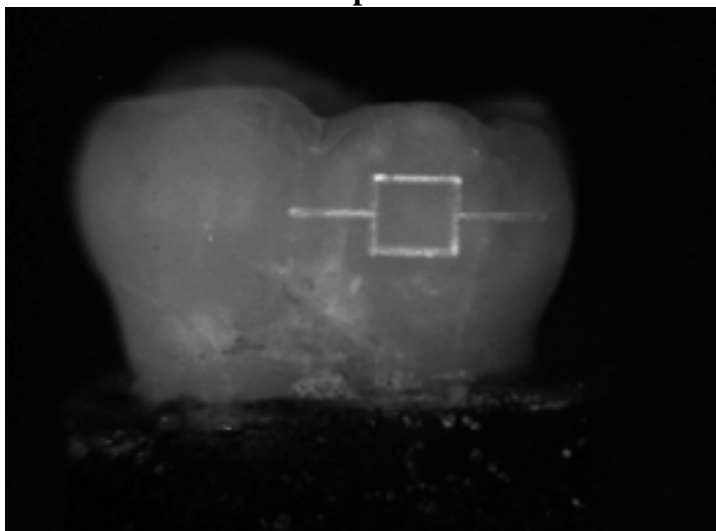


Visible



QLF

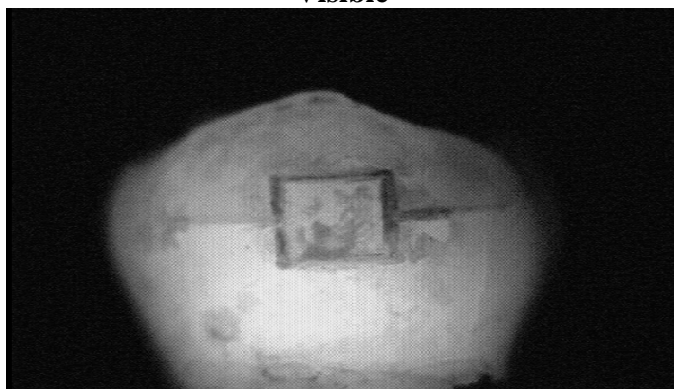
Sample 14



NIR Reflectance

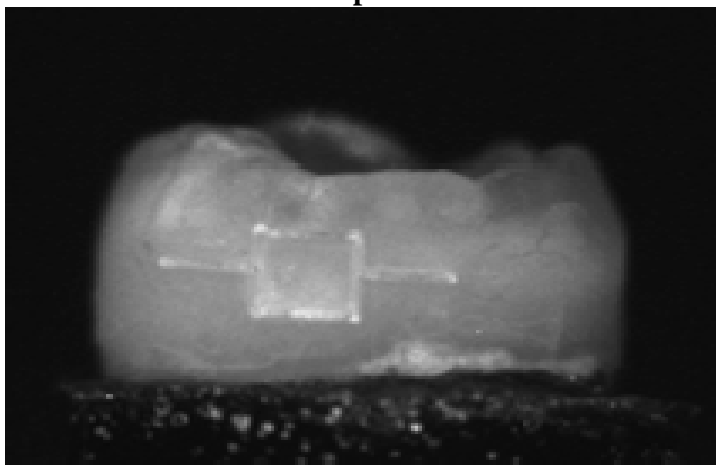


Visible



QLF

Sample 15



NIR Reflectance

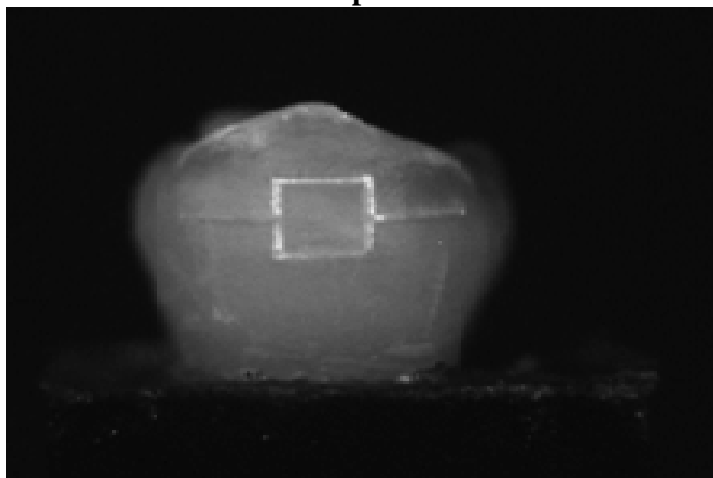


Visible



QLF

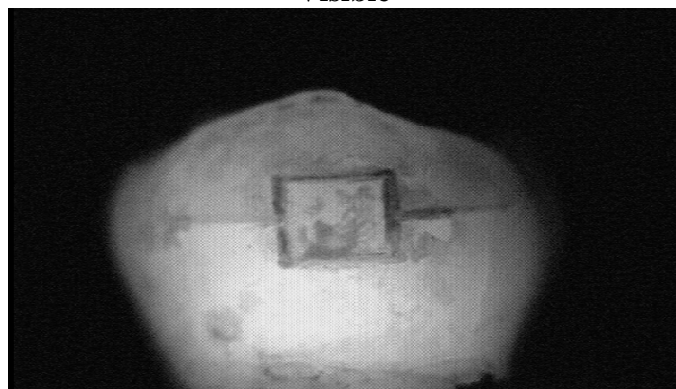
Sample 16



NIR Reflectance



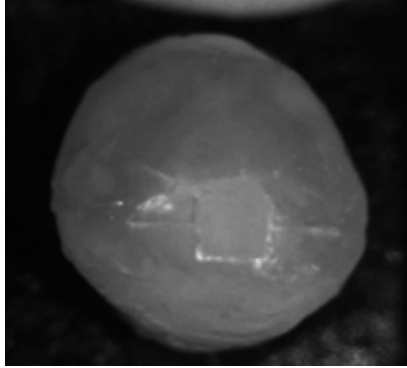
Visible



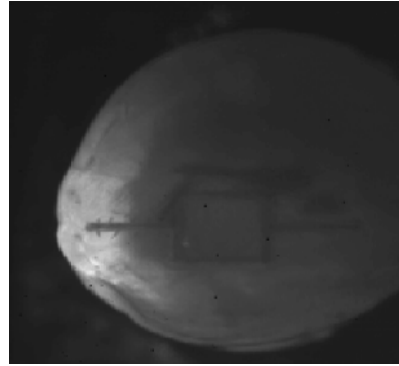
QLF

Appendix B: Occlusal Surfaces

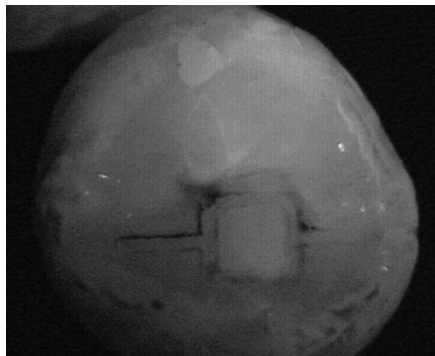
Sample 1



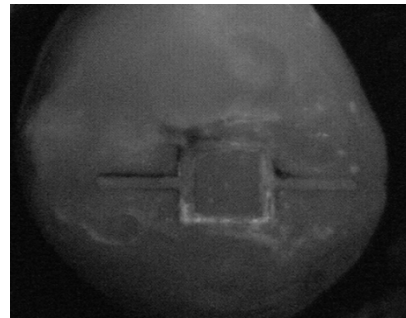
NIR Reflectance



NIR Transillumination

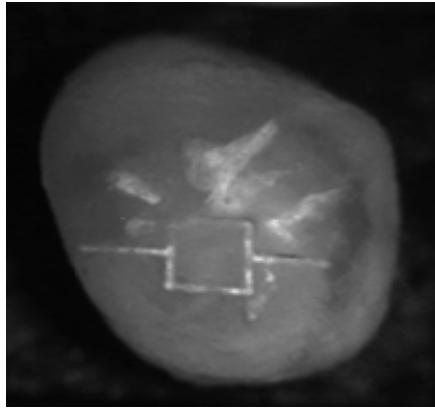


QLF

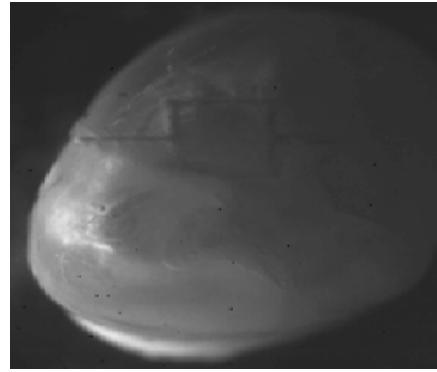


Visible

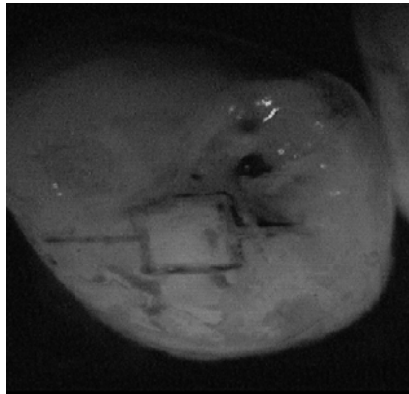
Sample 2



NIR Reflectance



NIR Transillumination

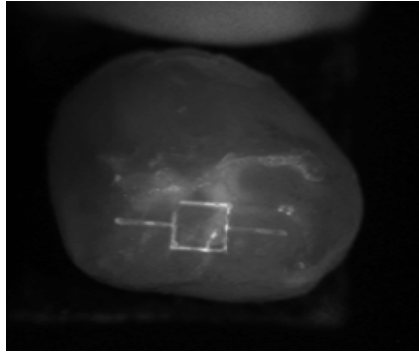


QLF

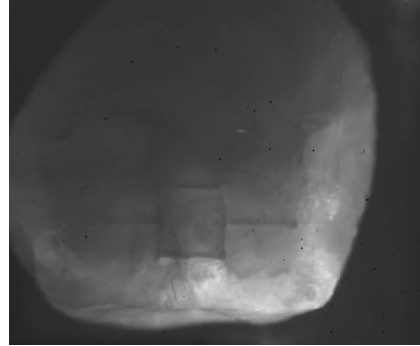


Visible

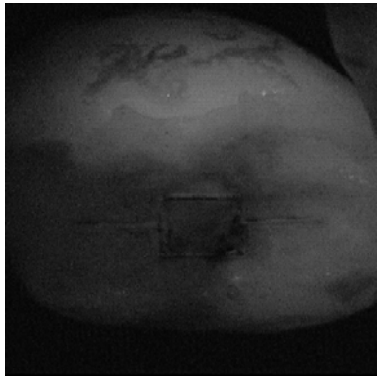
Sample 3



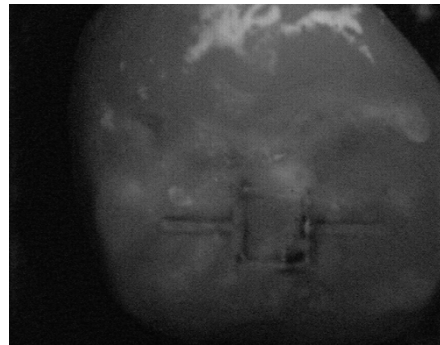
NIR Reflectance



NIR Transillumination

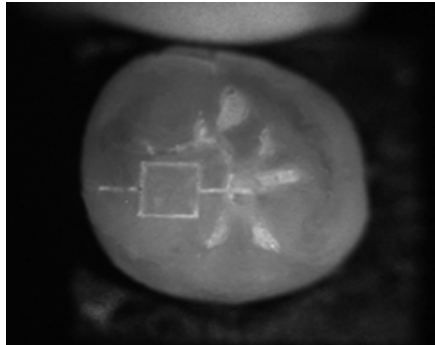


QLF

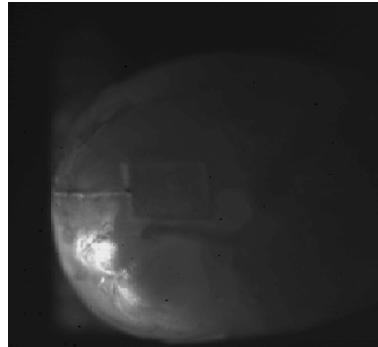


Visible

Sample 4



NIR Reflectance



NIR Transillumination

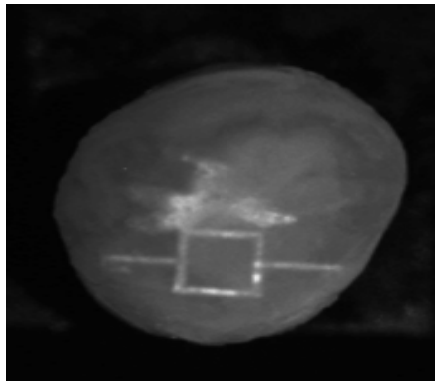


QLF

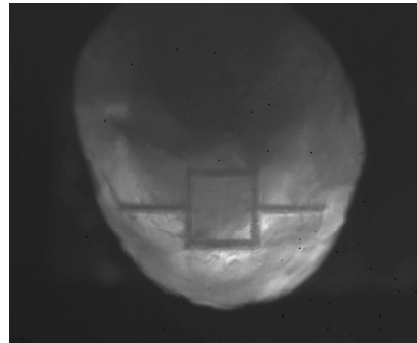


Visible

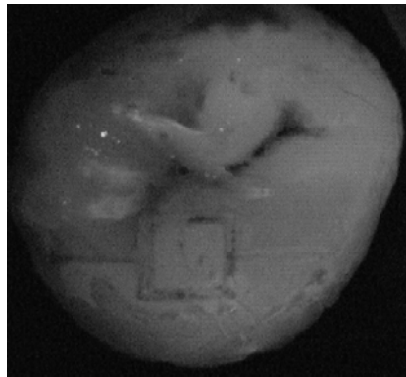
Sample 5



NIR Reflectance



NIR Transillumination

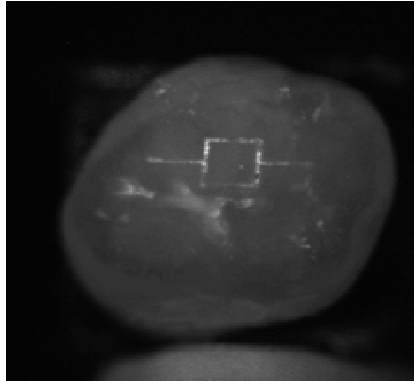


QLF

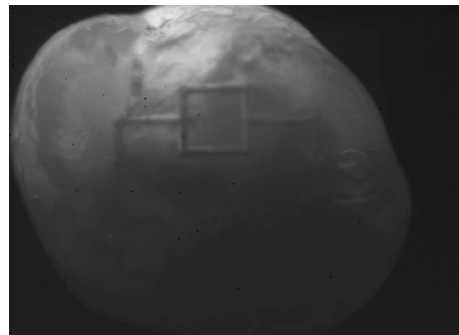


Visible

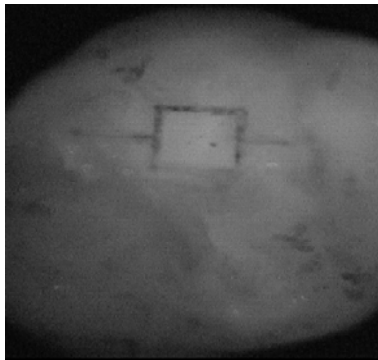
Sample 6



NIR Reflectance



NIR Transillumination

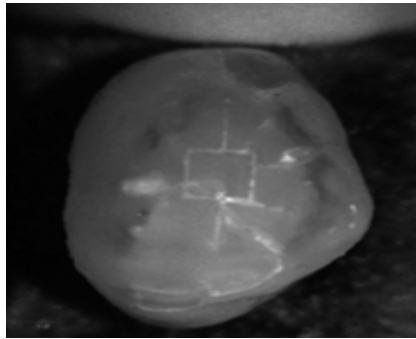


QLF

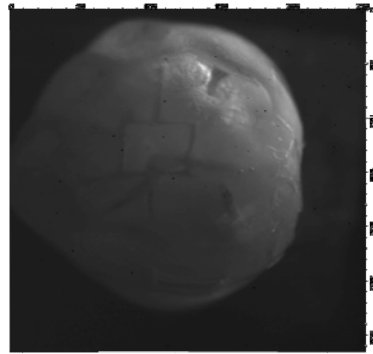


Visible

Sample 7



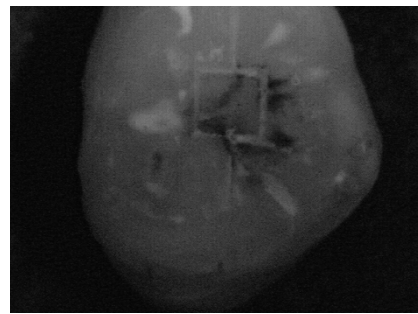
NIR Reflectance



NIR Transillumination

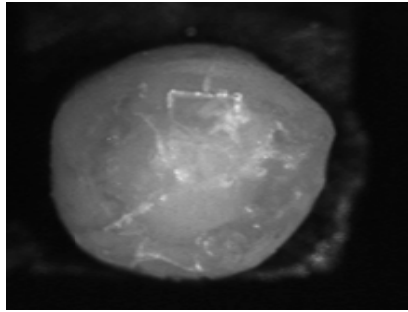


QLF

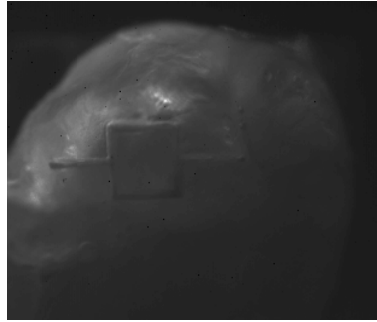


Visible

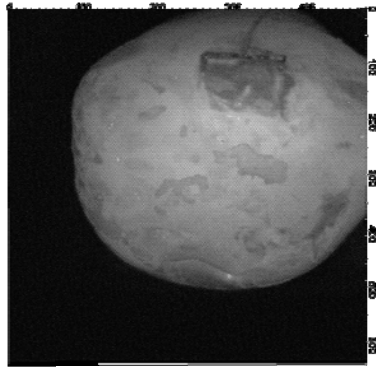
Sample 8



NIR Reflectance



NIR Transillumination

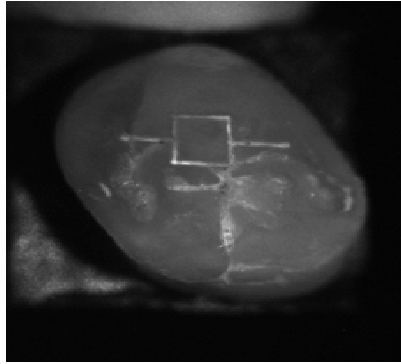


QLF

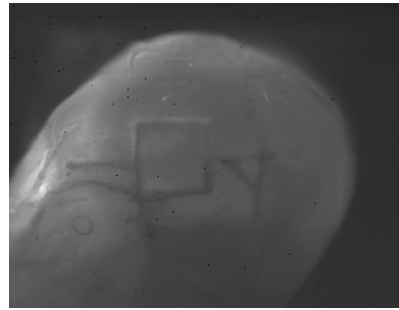


Visible

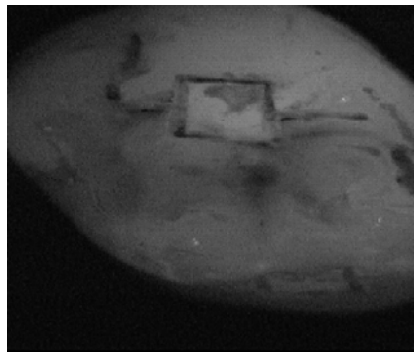
Sample 9



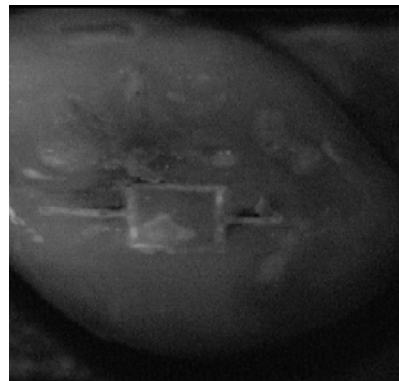
NIR Reflectance



NIR Transillumination

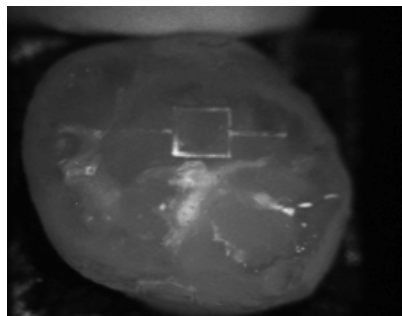


QLF

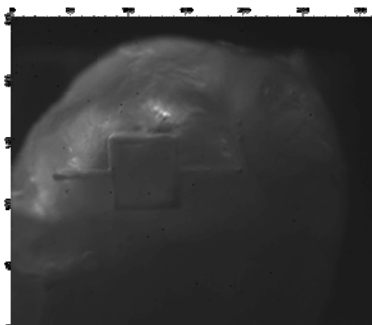


Visible

Sample 10



NIR Reflectance



NIR Transillumination

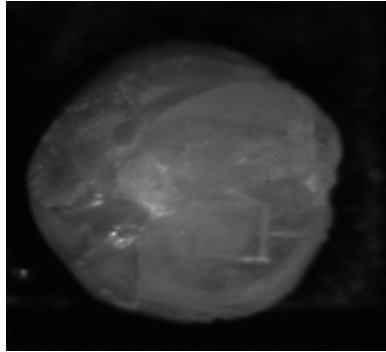


QLF

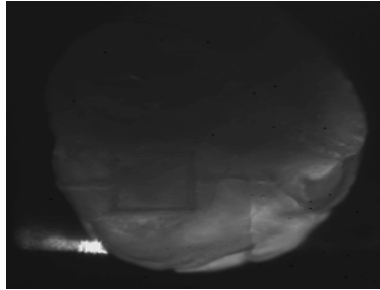


Visible

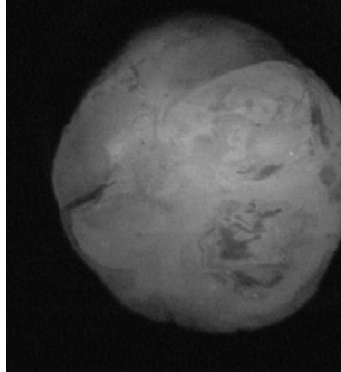
Sample 11



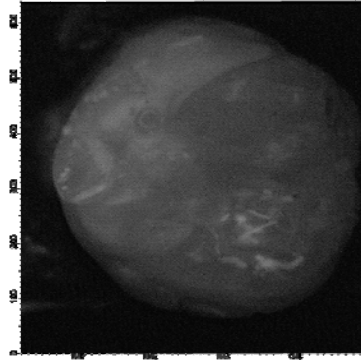
NIR Reflectance



NIR Transillumination

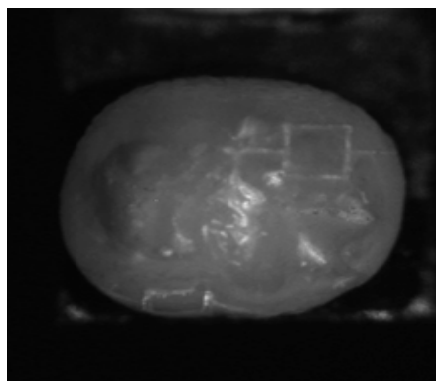


QLF

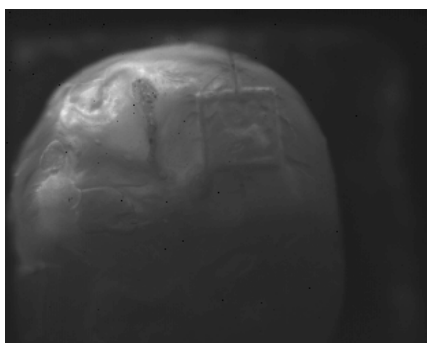


Visible

Sample 12



NIR Reflectance



NIR Transillumination

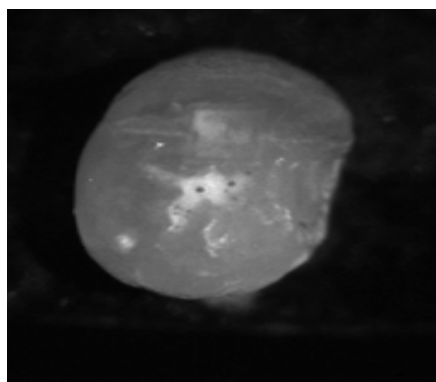


QLF

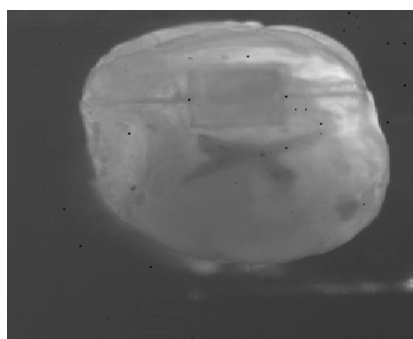


Visible

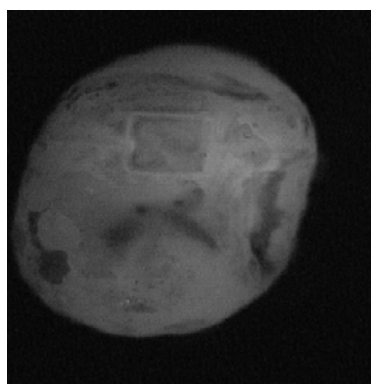
Sample 13



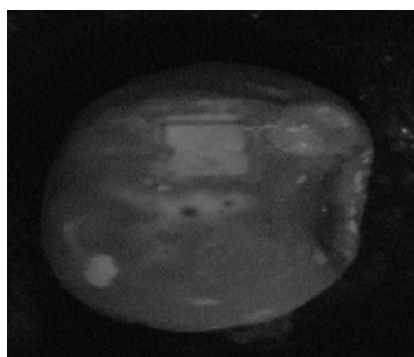
NIR Reflectance



NIR Transillumination

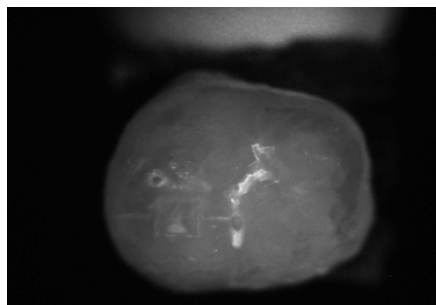


QLF

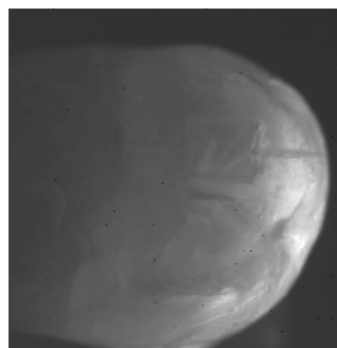


Visible

Sample 14



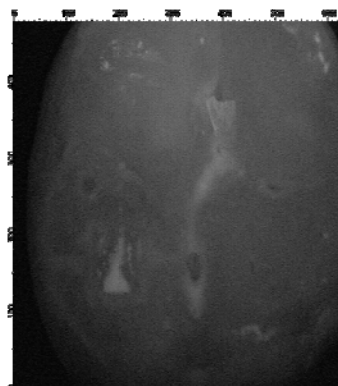
NIR Reflectance



NIR Transillumination

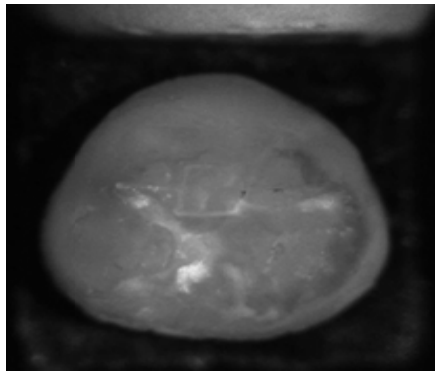


QLF

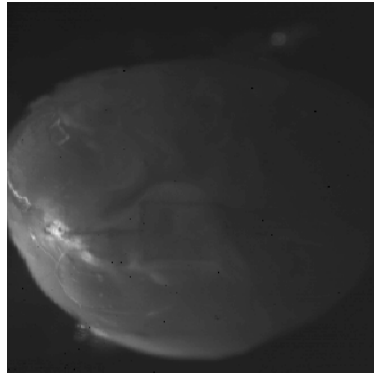


Visible

Sample 15



NIR Reflectance



NIR Transillumination

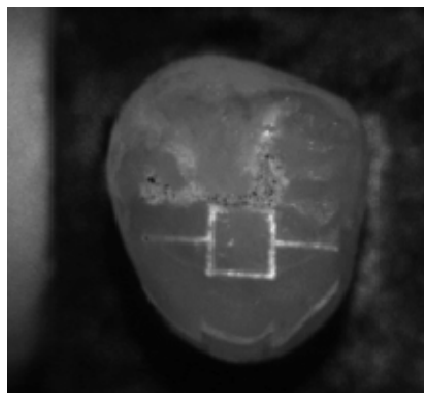


QLF

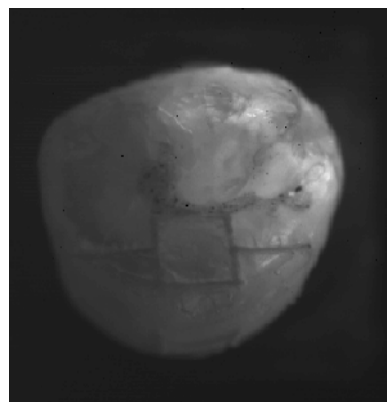


Visible

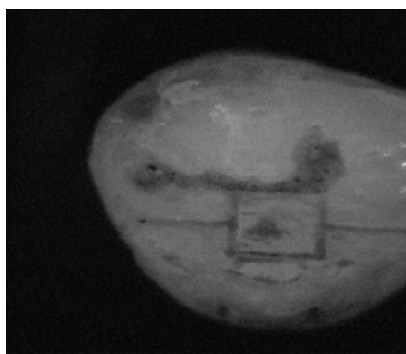
Sample 16



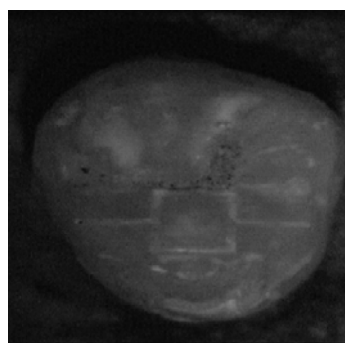
NIR Reflectance



NIR Transillumination



QLF



Visible

University of California, San Francisco

Publishing Agreement

It is the policy of the University to encourage the distribution of all theses, dissertations, and manuscripts. Copies of all UCSF theses, dissertations, and manuscripts will be routed to the library via the Graduate Division. The library will make all theses, dissertations, and manuscripts accessible to the public and will preserve these to the best of their abilities, in perpetuity.

Please sign the following statement:

I hereby grant permission to the Graduate Division of the University of California, San Francisco to release copies of my thesis, dissertation, or manuscript to the Campus Library to provide access and preservation, in whole or in part, in perpetuity.



6/10/10

Author Signature Date